



Prediction of Seismic Compression of Unsaturated Backfills

John S. McCartney, Ph.D., P.E., F.ASCE
Professor, Department of Structural Engineering
University of California San Diego

PEER Annual Meeting, Berkeley, CA
August 25, 2023



Research Team

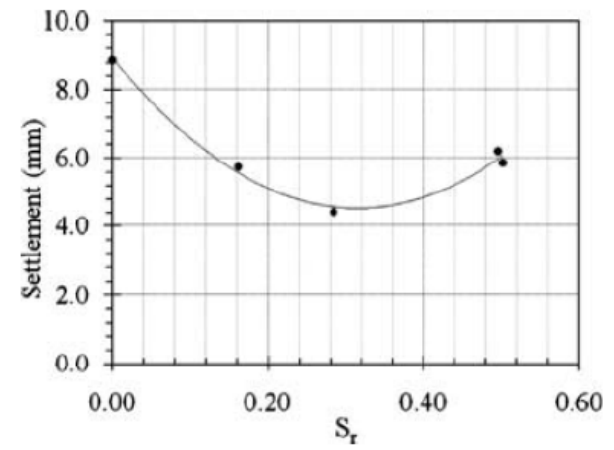
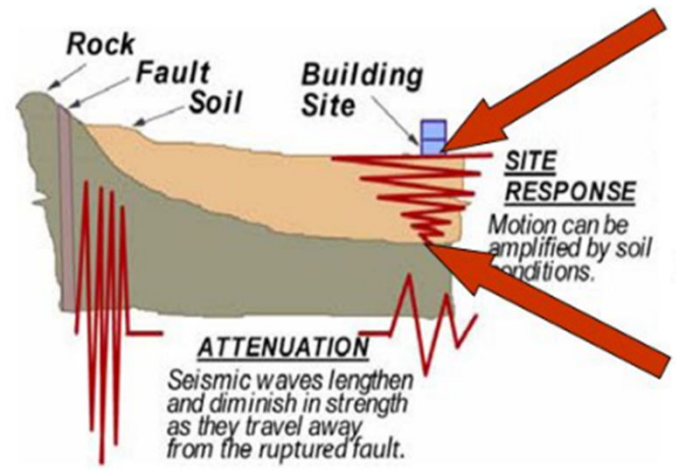
- Interests in this area stemmed from PhD studies of Majid Ghayoomi at CU Boulder
- Wenyong Rong, PhD from UCSD in 2020
 - Currently working for Mott McDonald
 - PhD research was focused on experimental evaluation of seismic compression of unsaturated soils
 - Performed a series of cyclic simple shear tests on medium dense sand under drained and undrained conditions
- Dellena Kinikles, MS from UCSD in 2022
 - Developed an elasto-plastic constitutive model for seismic compression of unsaturated soils





Seismic Compression of Unsaturated Soils

- Seismic compression is the accrual of *contractive* volumetric strains in soils due to cyclic shearing during earthquake events and has been recognized as a major cause of seismically-induced damage to buildings, pavements and other geotechnical structures (Stewart et al. 2004)
- May be important to consider in site response or serviceability analyses
- Research needs:
 - Build a database of cyclic shearing tests on unsaturated soils
 - Develop a physics-based methodology to understand the impacts of unsaturated conditions (initial degree of saturation, suction, etc.)



Ghayoomi et al. (2011)



Geotechnical Systems with Unsaturated Soils



Mechanically-stabilized earth walls



Road/rail embankments

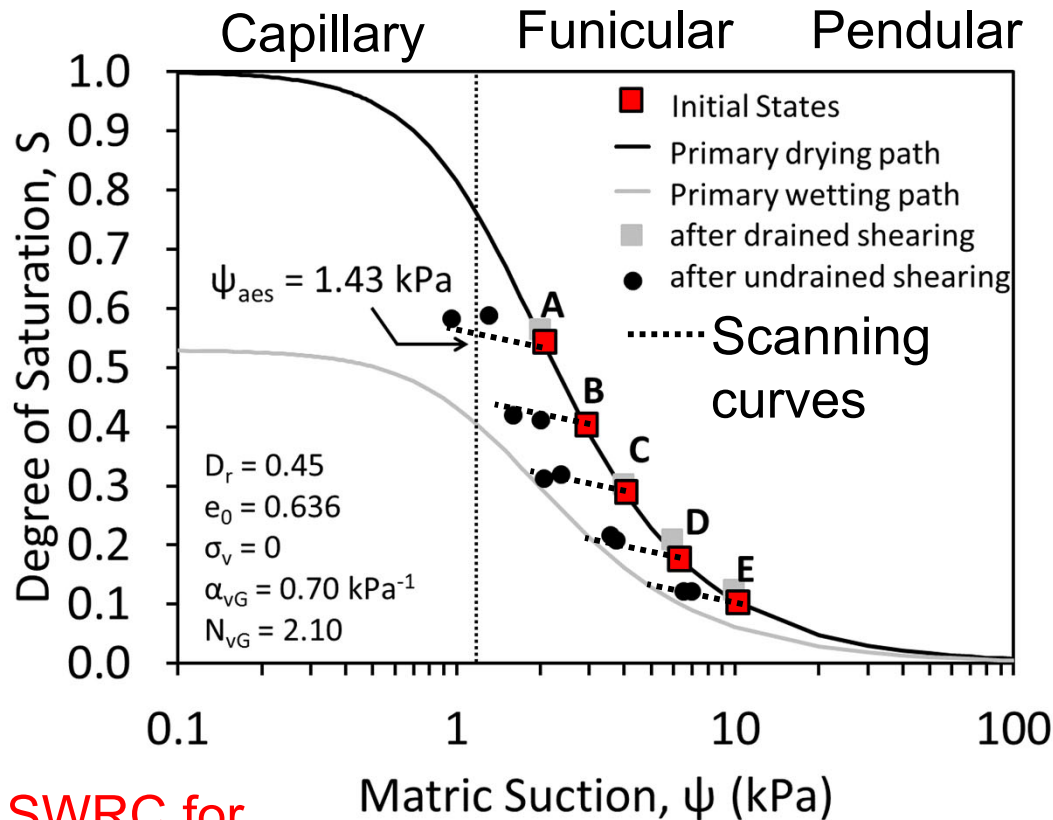


MSE Bridge Abutments

- Backfill in many geotechnical systems is intended to **remain in unsaturated conditions by design** (with appropriate drainage)
- Northridge earthquake report by Stewart et al. (1995) found that seismic compression of fills caused damages on the order of \$50,000 to \$100,000 per lot
- Seismic compression of backfill soils may be a key design factor as **small settlements may have a major effects on superstructure**
- While looser soils are expected to exhibit more seismic compression, backfill soils are usually initially dense due to compaction
 - **Dense soils may still show contractive strains during cyclic shearing**
 - Density may be lower near the face where deformations are critical



Soil Water Retention Curve (SWRC)



SWRC for
SW Sand
(Rong and
McCartney
2020)

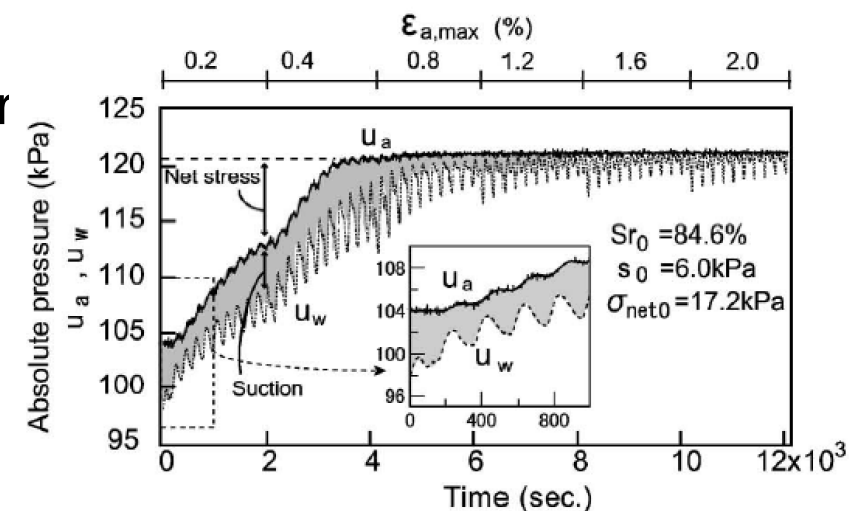
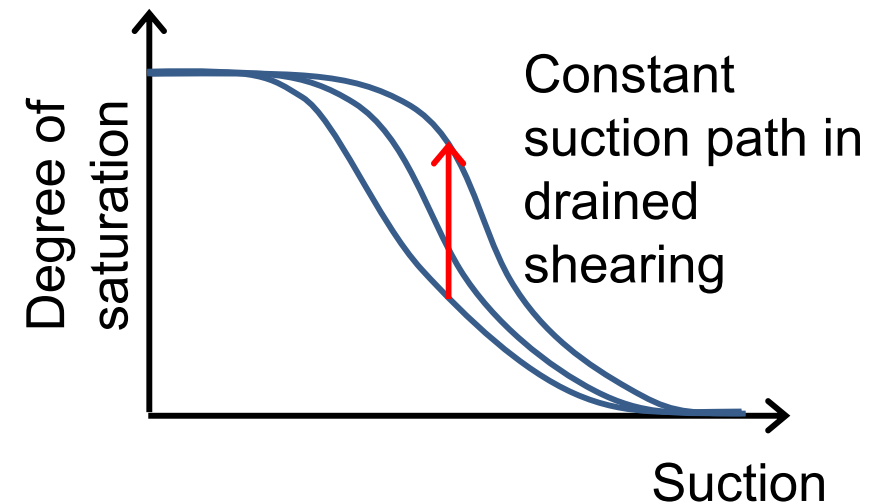
Matric Suction, ψ (kPa)
 u_a = Pore air pressure
 u_w = Pore water pressure
 $\psi = u_a - u_w$ = Matric suction
 S = Degree of saturation

- SWRC is the key relationship for both hydraulic and mechanical analyses
- Suction reflects the energy in the pore water with respect to free water
- SWRC depends on pore size distribution, particle shape, and soil-water interaction mechanisms
- *Funicular regime* is the focus of this study as this is where the *degree of saturation changes most with suction and where water and air can both be continuous*
- Hydraulic hysteresis:
 - Different primary wetting and drying paths
 - Soils will likely follow a wetting-path *scanning* curve during hydraulic hysteresis



Drainage Conditions During Cyclic Shearing

- Drained water and air (constant suction):
 - Occurs during slow cyclic shearing
 - SWRC of soil evolves with volume change as S increases with constant suction
- Undrained water and drained air:
 - May occur in relatively dry soils that are close to ground surface with a free air phase
 - Soil may become fully undrained when air is expelled depending on shearing rate
- Undrained water and undrained air (focus):
 - Occurs during fast cyclic shearing like earthquakes, confined layers or layers with occluded air phase
 - Both u_a and u_w will change

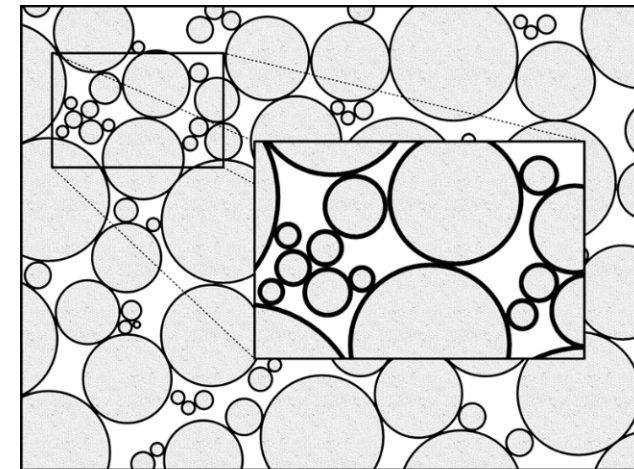


Fully Undrained: Unno et al. (2008)

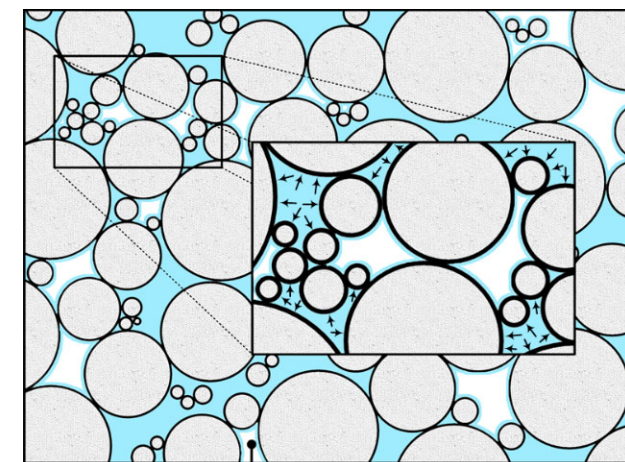


Hydromechanics of Seismic Compression

- Voids filled with pore **air** will collapse/densify leading to volume changes
- Pore fluids (air and water) will **pressurize** during undrained cyclic shearing
- Suction changes depend on **differential pressurization** of pore air and water
- **Degree of saturation will evolve** with changes in soil volume for both drained/undrained cases
- Degree of saturation is a key variable that partitions the quantity of air and water filled voids as well as the **equivalent bulk modulus** that can be used to determine pore fluid pressurization
- Both degree of saturation and matric suction affect the **effective stress that governs elastic moduli** and elastic strains



$S = 0$



Pore Air

$S = S_1$



Effective Stress in Unsaturated Soils

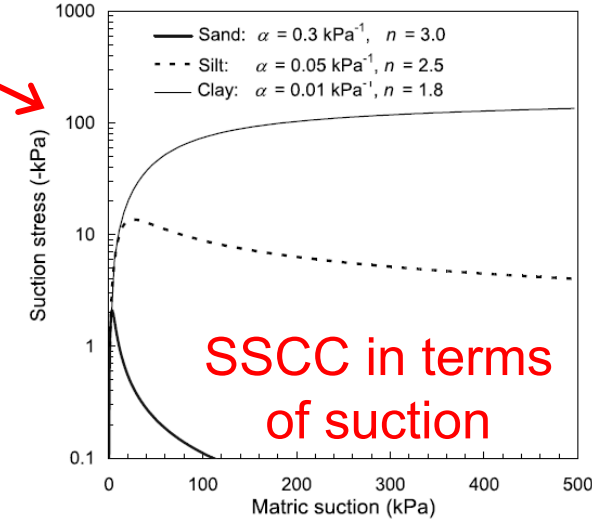
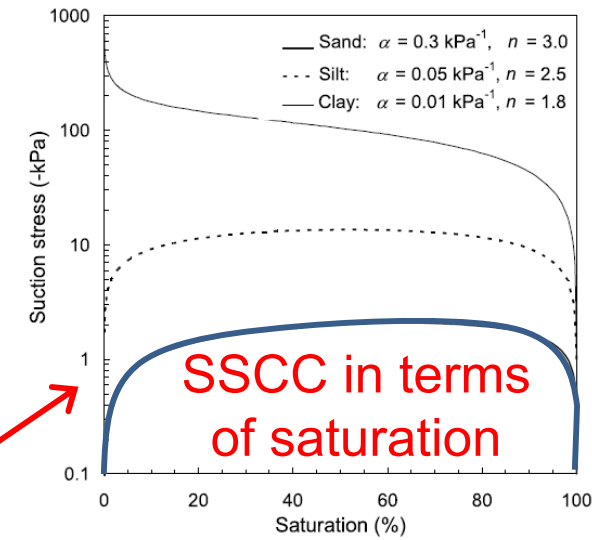
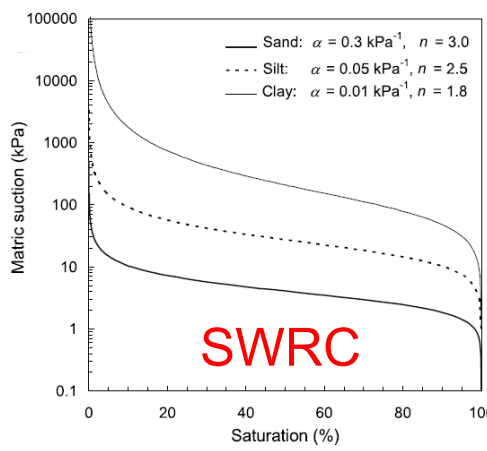
- Effective stress definition (Bishop 1959):

$$\sigma'_{ij} = (\sigma_{ij} - u_a \delta_{ij}) + \chi(u_a - u_w) \delta_{ij}$$
- Suction stress concept (Lu and Likos 2006):

$$\sigma'_{ij} = (\sigma_{ij} - u_a \delta_{ij}) + \sigma_s \delta_{ij}$$
- SWRC can be integrated into suction stress to define the suction stress characteristic curve, SSCC (Lu et al. 2010):

$$\sigma_s = S_e(u_a - u_w)$$

$$S_e = \left(\frac{S - S_{res}}{1 - S_{res}} \right) = \left[\frac{1}{1 + (\alpha_{vG}(u_a - u_w))^{N_{vG}}} \right]^{\frac{1}{1 - N_{vG}}}$$

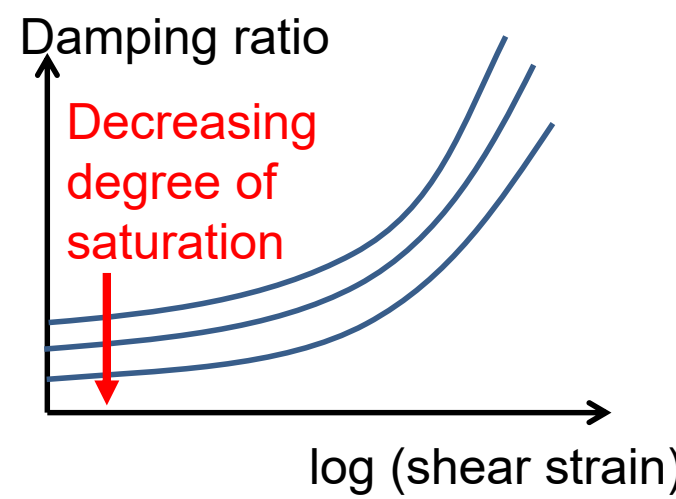
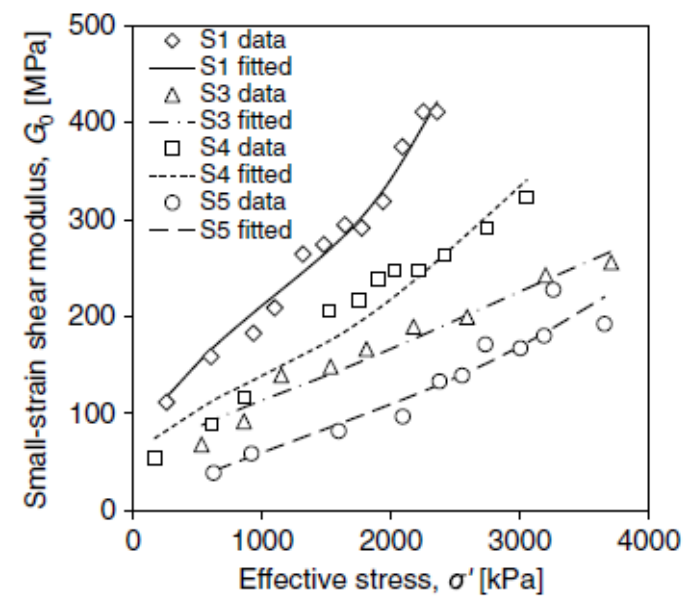


Focus here on soils with a sand-like SWRC and SSCC



Role of Effective Stress in Seismic Compression

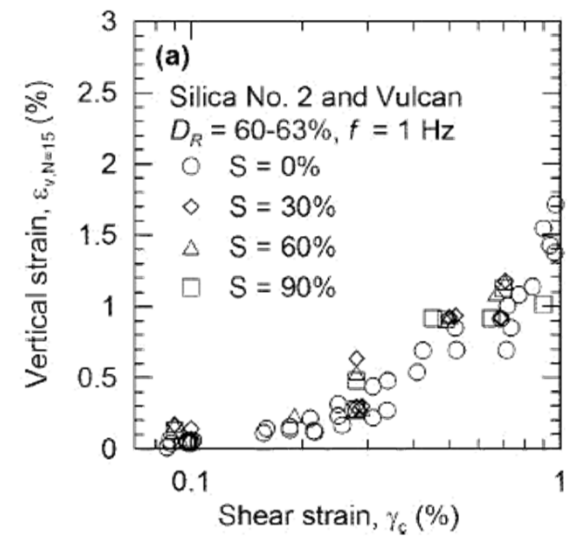
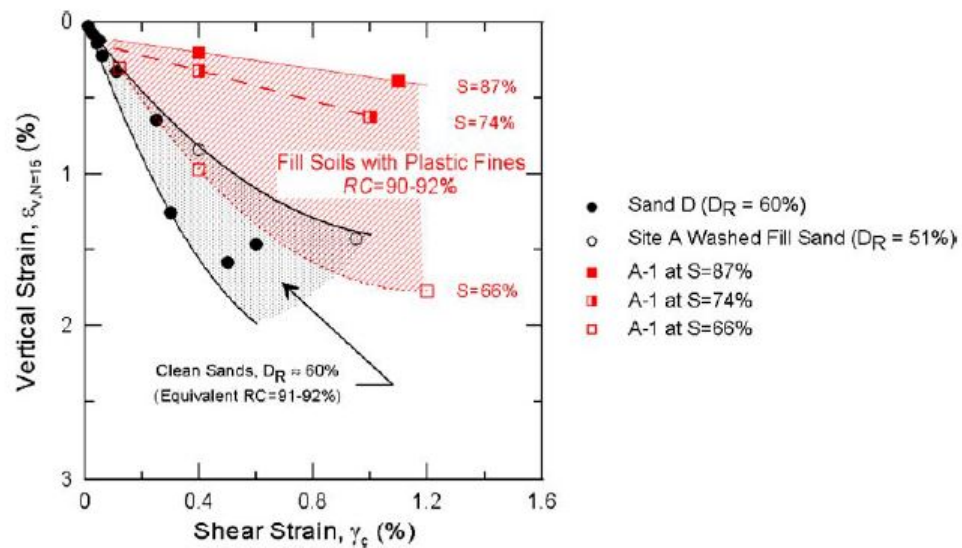
- Effective stress is expected to evolve during drained or undrained seismic compression
- Effective stress is *directly proportional* to the elastic shear/bulk moduli and damping ratio, which govern the cyclic response
- Effective stress is only directly proportional to *elastic* volume changes through Hooke's law
- Phenomena like seismic compression are *elasto-plastic* where suction has independent effects on effective stress and yield stress
- Knowledge of effective stress changes alone is critical but not sufficient for modeling of seismic compression





Seismic Compression of Unsaturated Soils

➤ **Wang et al. (2004)** and **Duku et al. (2008)** found that the degree of saturation was important for soils with moderately plastic fines, but trends with degree of saturation were unclear

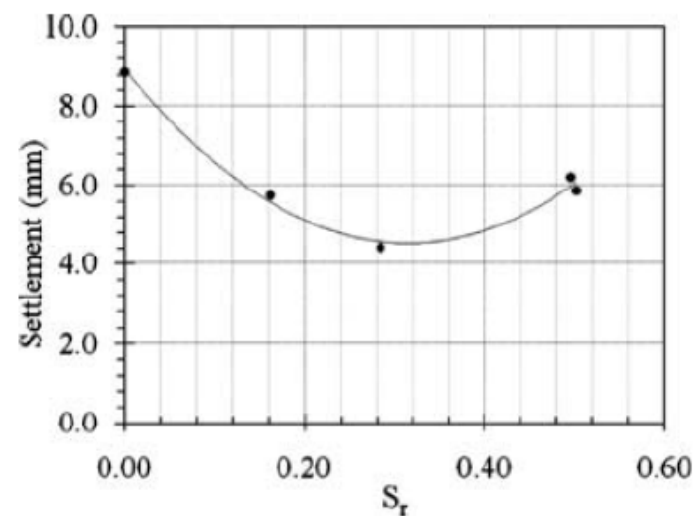
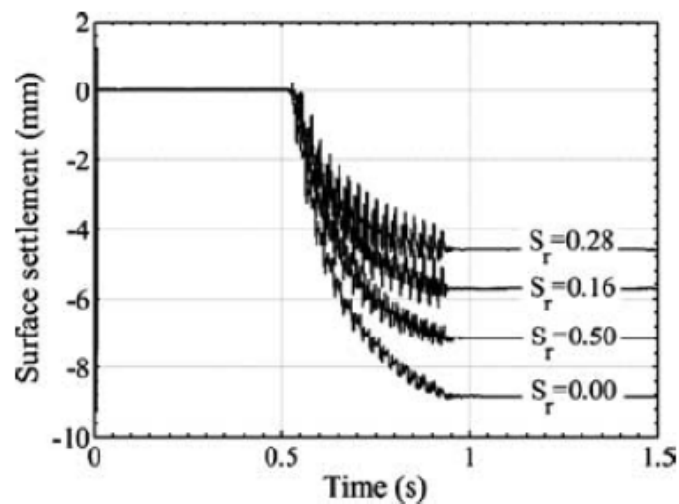


Comments: Unsaturated specimens were prepared by tamping and kneading wet soils to target relative densities, leading to uncertainties associated with **compaction-induced soil structure**



Seismic Compression of Unsaturated Soils

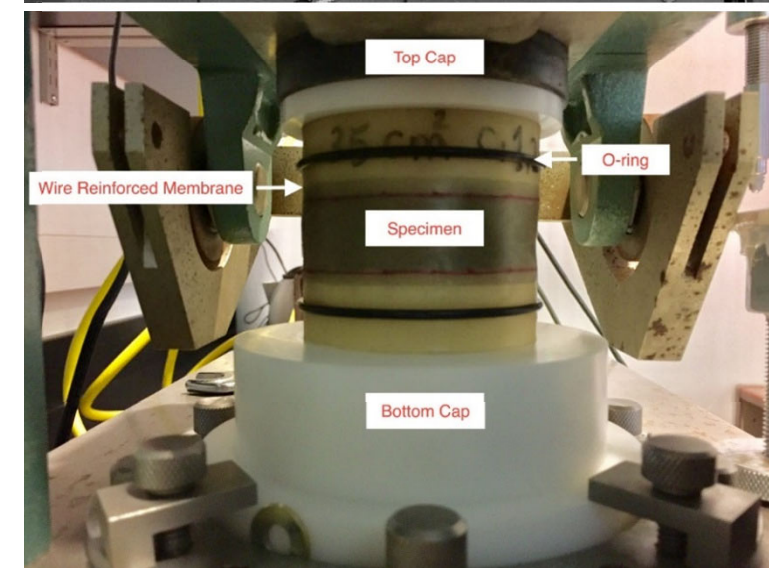
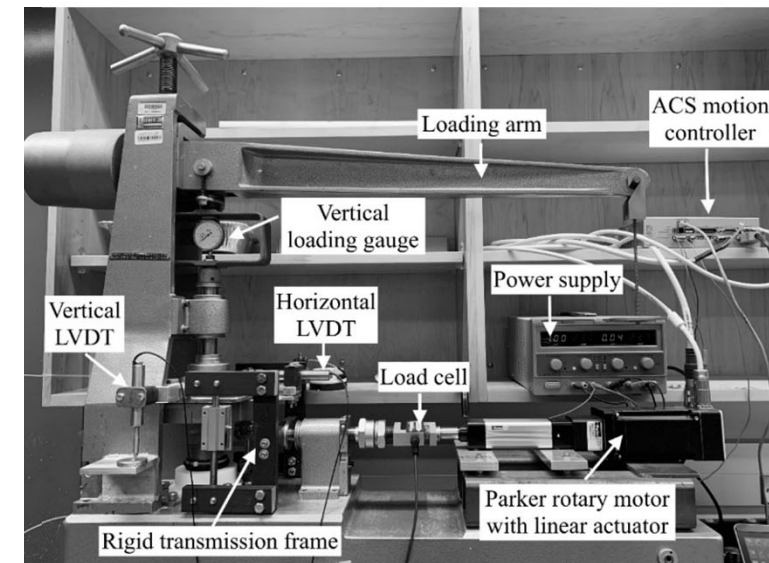
- Ghayoomi et al. (2011) performed a set of centrifuge tests on unsaturated sand layers with uniform suction along the depth, and found the lowest seismic compression corresponds to the condition with the maximum value of suction stress



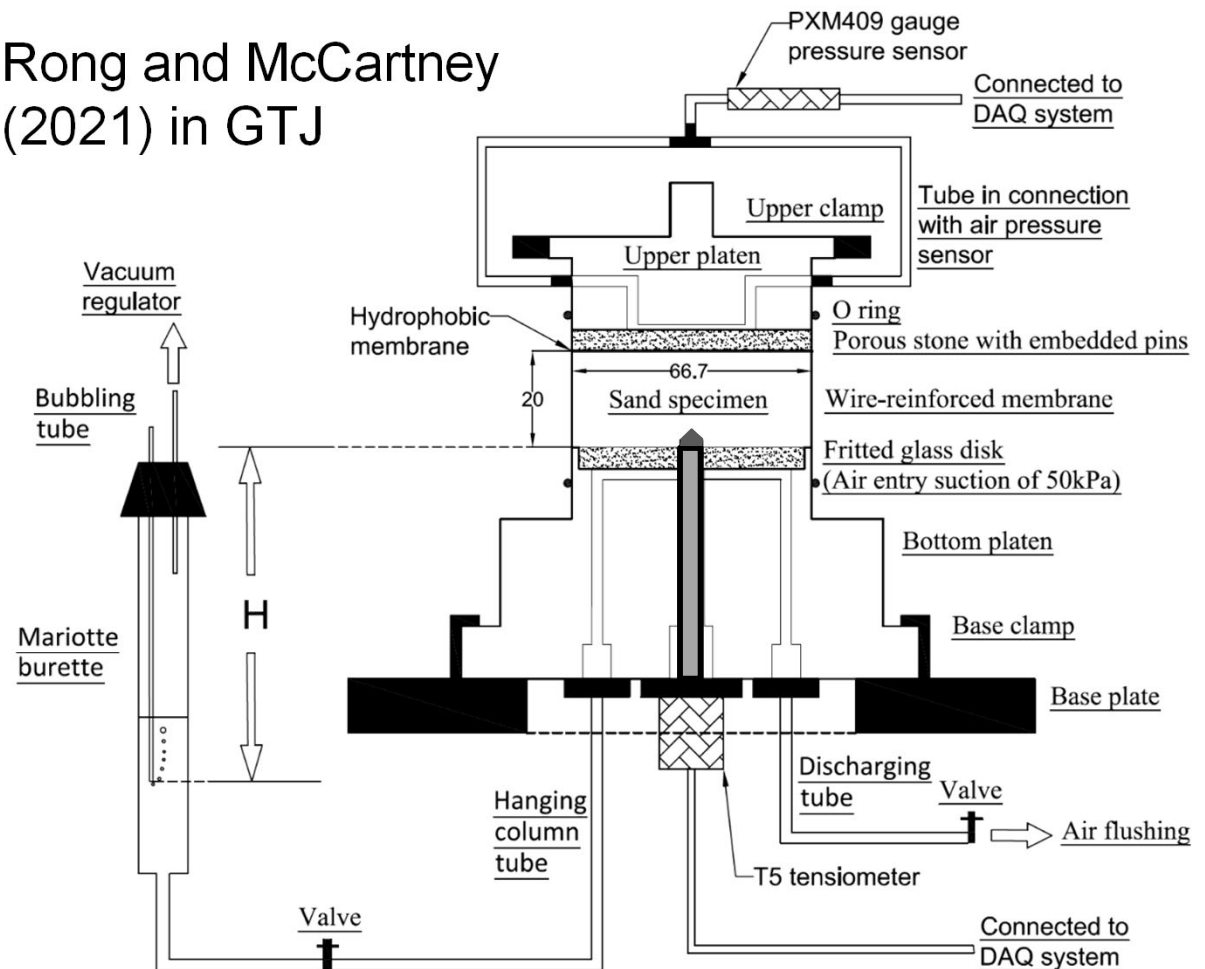
Comments: Drainage conditions of the pore water and pore air are unknown in centrifuge tests, and their role on the seismic compression of unsaturated sand was not investigated



Seismic Compression of Unsaturated Soils



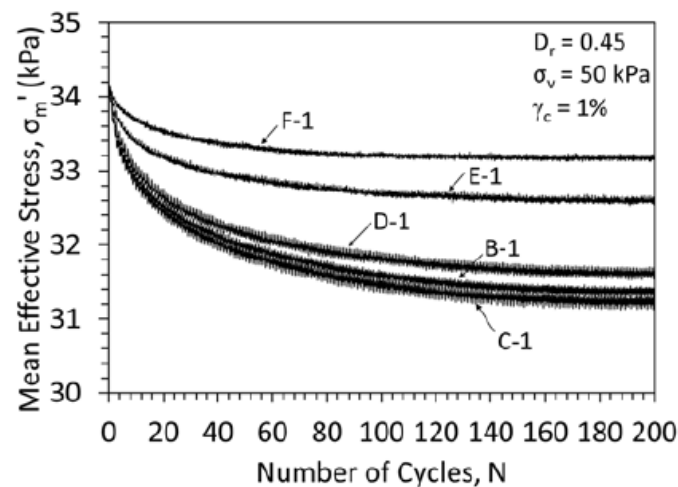
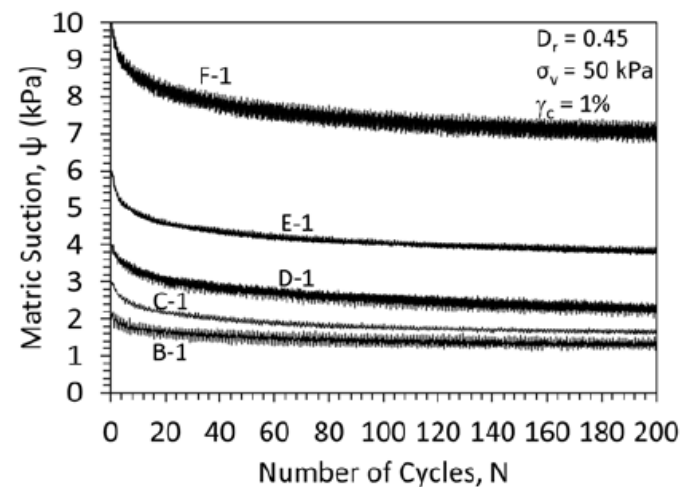
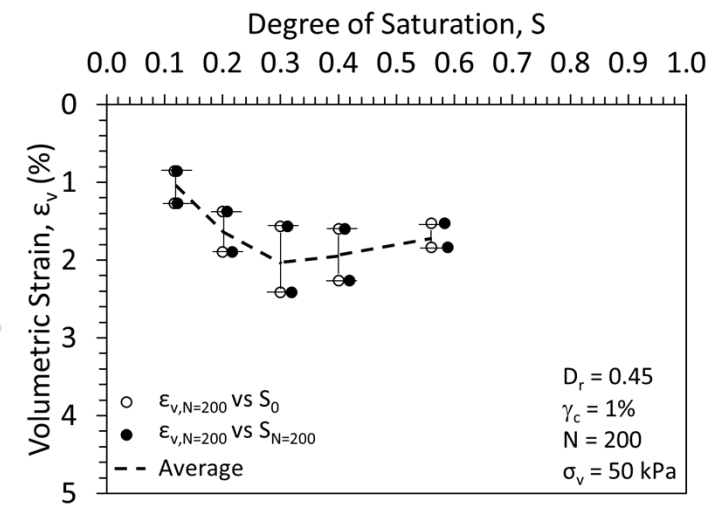
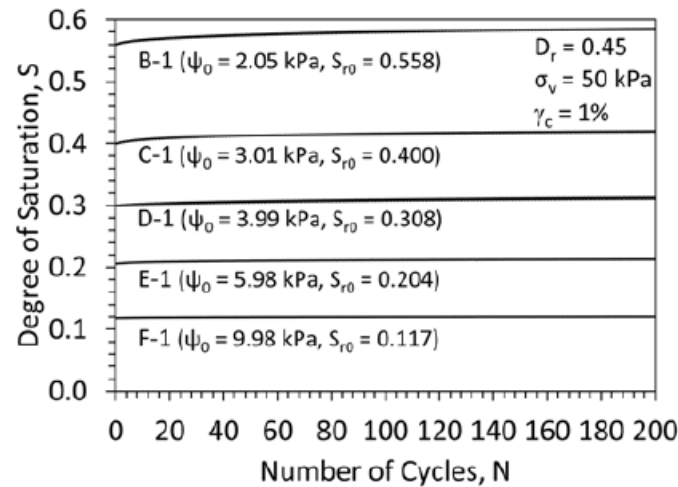
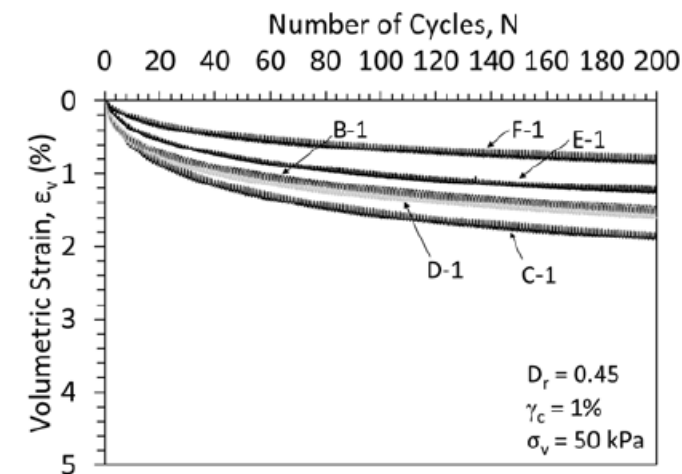
Rong and McCartney
(2021) in GTJ



Specimen housing with separate
measurements of pore water pressure and
pore air pressure (units: mm)



Example Experimental Results (Undrained)



Opposite trend with S_0 from Ghayoomi et al. (2011), possibly due to combined effects of pore fluid pressurization and effective stress effects



Empirical Approach to Estimate Seismic Compression

Yee, Stewart,
Tokimatsu (2011)

$$(\varepsilon_v)_{N=15} = a(\gamma - \gamma_{tv})^b$$

D_R (%)	w (%)	σ_v (kPa)	a	b	γ_{tv} (%)	a^{**}
32-43	6-7	100	1.91	1.34	0.03	1.88
28-42	17-18	50	2.50	1.11	0.038	2.56
31-41	17-19	100	2.27	1.33	0.034	2.23
33-43	17-18	200	1.86	1.42	0.03*	1.79
31-41	17-18	400	1.95	1.54	0.044	1.86
55-58	6-9	100	1.24	1.28	0.03*	1.22
56-67	16-17	100	1.42	1.33	0.03*	1.40
62-62	17-18	400	0.82	1.39	0.05*	0.63

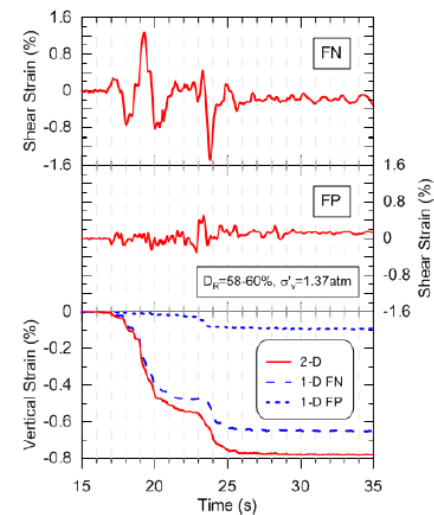
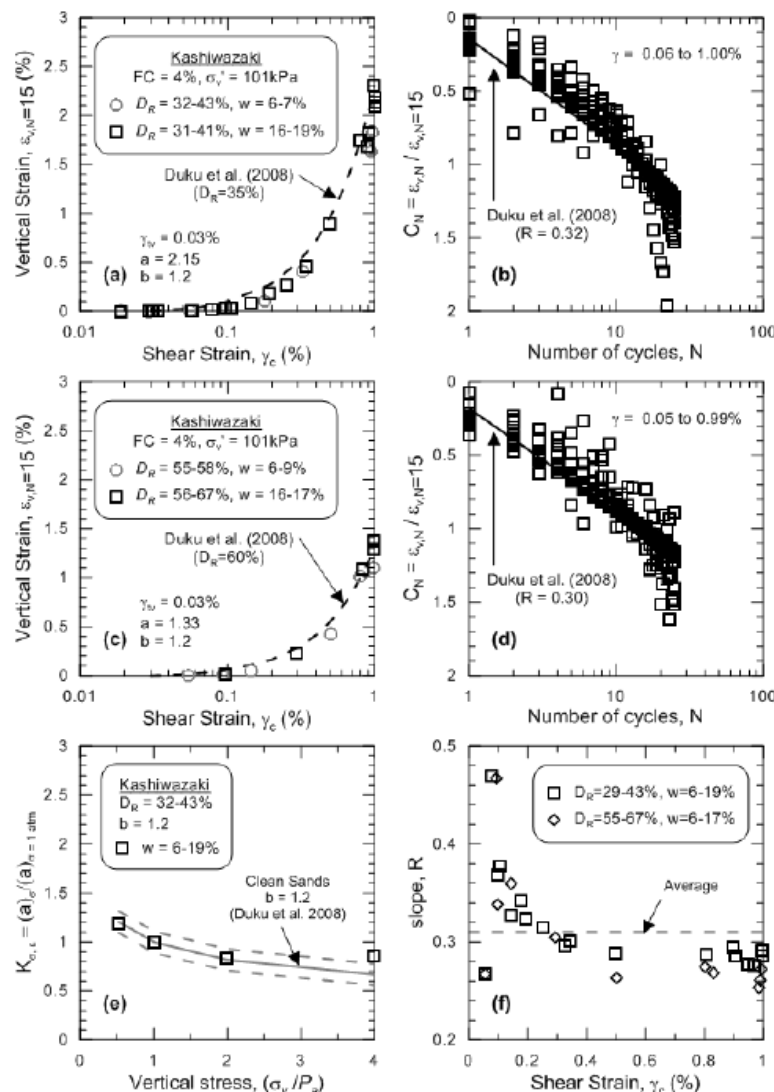
* assumed values due to lack of data for γ_{tv}

** b fixed at 1.2

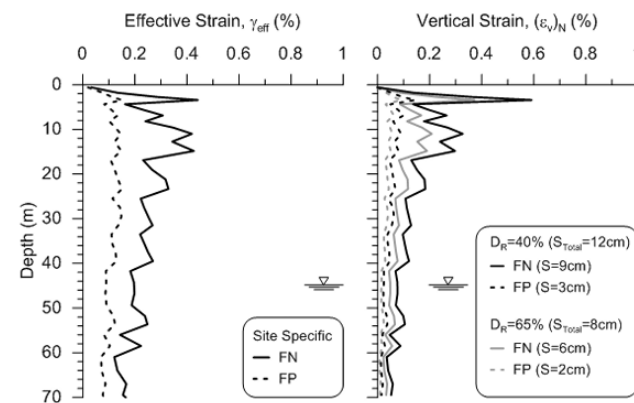
$$C_N = R \ln N + c = (\varepsilon_v)_N / (\varepsilon_v)_{N=15}$$

$$\gamma_{eff}(z) = 0.65 \times \gamma_{max}(z)$$

$$\varepsilon_v(z) = (a \times K_{\sigma, \varepsilon}(z)) (\gamma_{eff}(z) - \gamma_{tv})^b \times C_N$$



Simple Shear Validation



Field Application



Ghayoomi et al. (2013) Methodology for Seismic Compression of Unsaturated Sands

- Volumetric strain of unsaturated sand during earthquake shaking by incorporating unsaturated effects into empirical relationships for:
 - (1) Compression of air-filled voids from Tokimatsu and Seed (1987)
 - Rearrangement of particles
 - Restraining effects of matric suction
 - (2) Consolidation due to dissipation of excess pore pressure from Ishihara and Yoshimine (1992)
 - Increase in degree of saturation
 - Local/global increases in excess pore water pressure
- Methodology assumes that these terms are additive, and incorporates effects of unsaturated conditions into the definitions of both terms:

$$\varepsilon_v = \varepsilon_{v-compression} + \varepsilon_{v-consolidation}$$



Ghayoomi et al. (2013) Methodology for Seismic Compression of Unsaturated Sands

$$\varepsilon_{v-compression} = f(\gamma_e, N, D_r, S_r)$$

Combine empirical relationship between SPT blow count and relative density of Tokimatsu and Seed (1987) with the empirical relationship between volumetric strain versus number of cycles proposed by Pradel (1998), and **add a linear reduction factor** for the degree of saturation:

$$\varepsilon_{v-compression} = \gamma_e \left(\frac{\left(\frac{D_r}{0.15} \right)^2}{20} \right)^{-1.2} \left(\frac{N}{15} \right)^{0.45} (1 - S_r)$$

D_r = relative density

γ_e = effective shear strain

N = number of cycles

S_r = degree of saturation

Tokimatsu and Seed (1987)

Pradel (1998)

Stewart and Whang (2003)

Iterative approach is used to obtain the equivalent shear strain using the average induced shear stress and the shear modulus reduction curve that employs an effective-stress-based small strain shear modulus



Ghayoomi et al. (2013) Methodology for Seismic Compression of Unsaturated Sands

$$\varepsilon_{v-consolidation} = f(r_u, D_r, \sigma, S_r)$$

- Pore pressure ratio, r_u induced by earthquake shaking
- Relative density, D_r Lee and Albaisa (1974)
- Overburden stress, σ Tokimatsu and Seed (1987)
- Degree of saturation, S_r Wu and Seed (2004)

$$\varepsilon_{v-consolidation} = \varepsilon_{v-liquefied}(r_u)^{2.25} \quad \text{Lee and Albaisa (1974)}$$

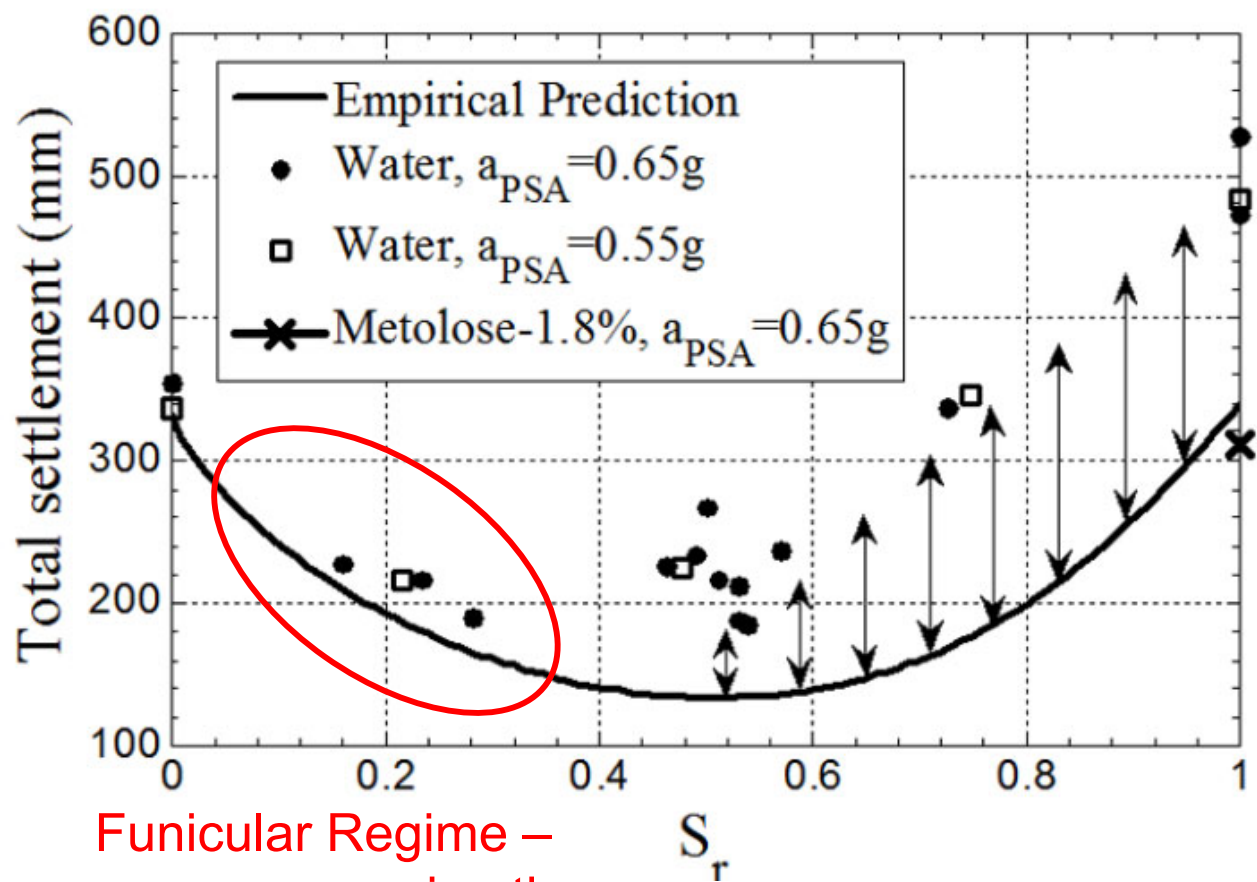
$$r_u = r_{u-sat} S_r^n \quad \text{Yoshimi et al. (1989)}$$

$$r_{u-sat} = 1/2 + 1/\pi \sin^{-1} \left(2 \left(\frac{N}{N_{L-sat}} \right)^{1/\alpha} - 1 \right) \quad \text{Kramer (1998)}$$

Estimate $\varepsilon_{v-liquefied}$ from empirical relationships of Tokimatsu and Seed (1987) or Wu and Seed (2004)



Ghayoomi et al. (2013) Methodology for Seismic Compression of Unsaturated Sands



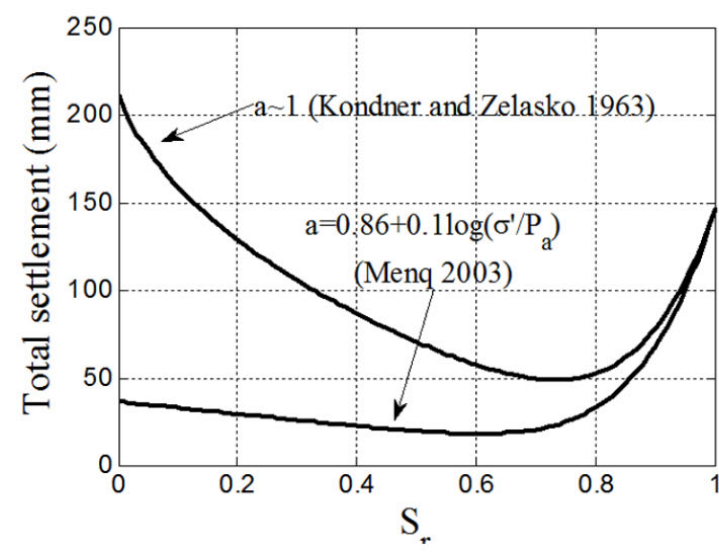
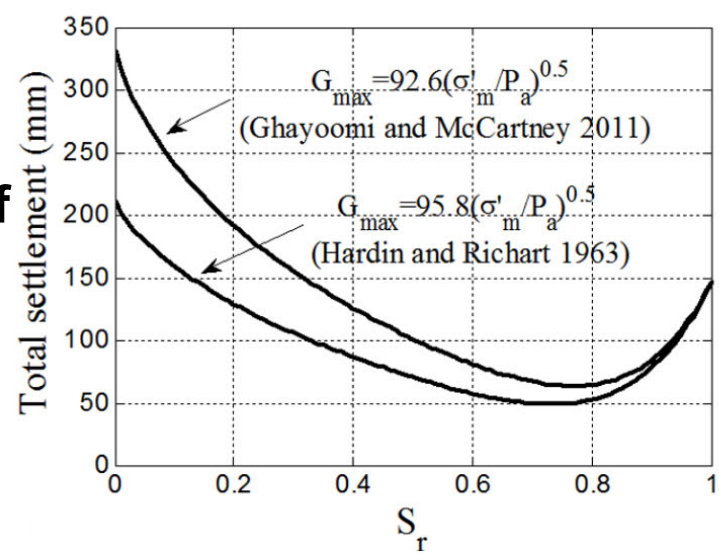
Funicular Regime –
more compression the
drier the soil is initially

- Comparisons of empirical methodology and results from centrifuge shaking table tests (Prototype scale)
- Reasonable prediction for low degrees of saturation
- Methodology under-predicts settlements at higher degrees of saturation, potentially due to partial drainage during shaking and scaling issues with pore fluid



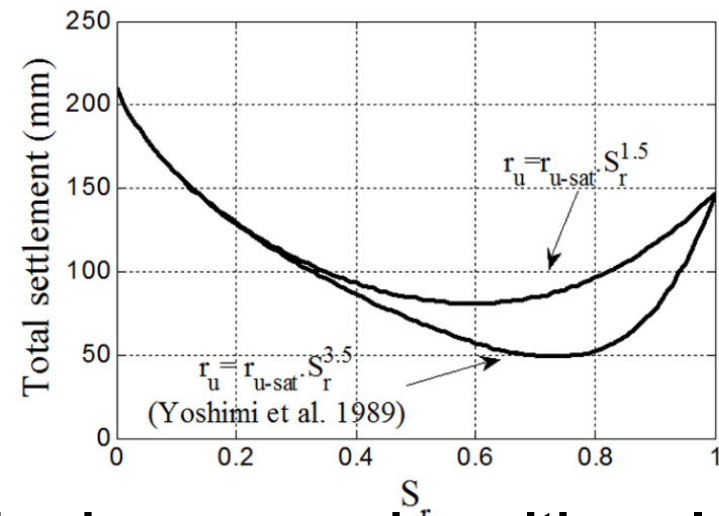
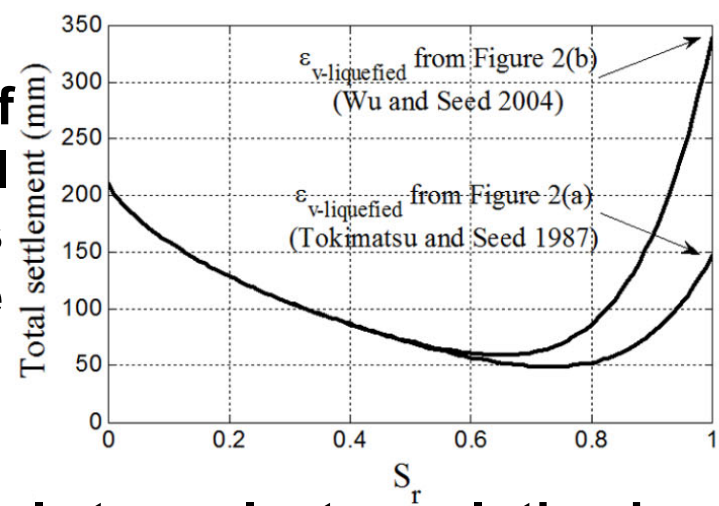
Issues with Ghayoomi et al. (2013) Model

Choice of models for G_{max}



Choice of models for the shear modulus reduction curve, exponent a

Choice of empirical relations to define $\epsilon_{v-liquefied}$



Choice of exponent n to define degree of saturation effects on pore water pressure ratio

Not simple to evaluate evolution in seismic compression with cycles of shearing

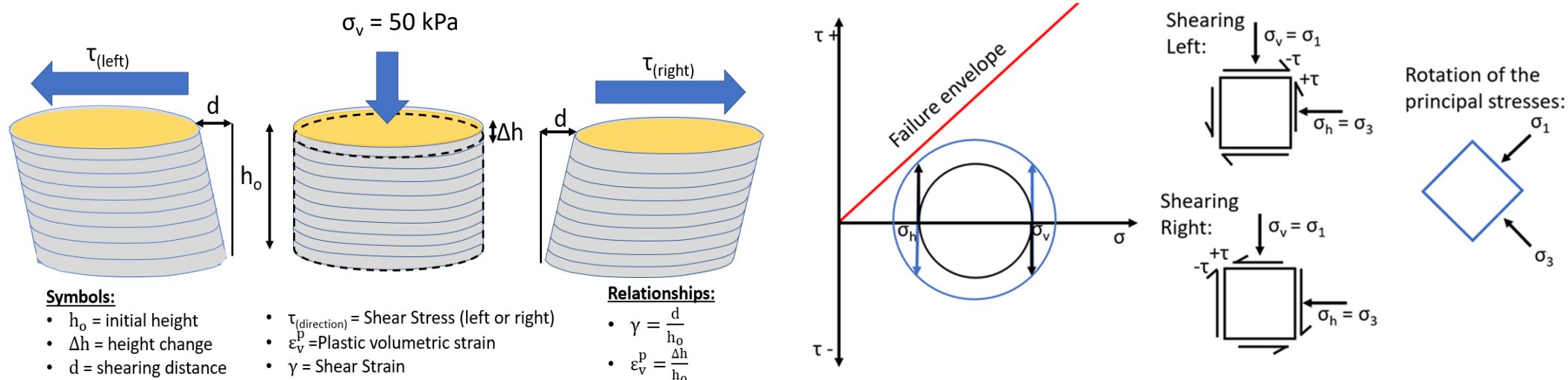


Hydro-mechanical Constitutive Model for Cyclic Shearing of Unsaturated Sands

- Key features of model:
 - Based on elasto-plastic stress-strain concepts of the UBCSAND model
 - Formulated using the effective stress for unsaturated soils by Lu et al. (2010)
 - Considers the plastic response caused by cyclic shearing (shear-induced volume change and associated degree of saturation changes)
 - Considers hydro-mechanical coupling effects on pore air pressure using a combination of Boyle's law and Henry's law
 - Estimates pore water pressures independently using SWRC scanning path
 - Consider the stress-dependency of the elastic properties of unsaturated soils
- Key assumptions:
 - Air in the pores is assumed to be an ideal gas obeying Boyle's and Henry's laws
 - Air and water phases are assumed to be continuous
 - Developed shear stress ratio is assumed to follow a hyperbolic relation with the plastic shear strain, similar to those adopted by Duncan and Chang (1970)



Cyclic Simple Shear Stress State



- Cylindrical wire housing resists any radial expansion allowing for K_o conditions to be valid
- Shearing stresses act to the LEFT or RIGHT during cyclic shearing corresponding to a rotation of the principal stresses with no change in mean stress



UBCSAND – Simplified Elasto-Plastic Model for Cyclic Shearing of Sands (Beatty & Byrne 2011)

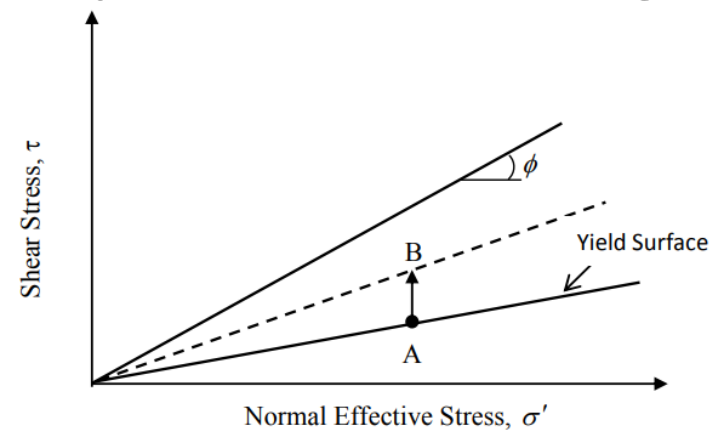


Figure 1. Yield surface in UBCSAND.

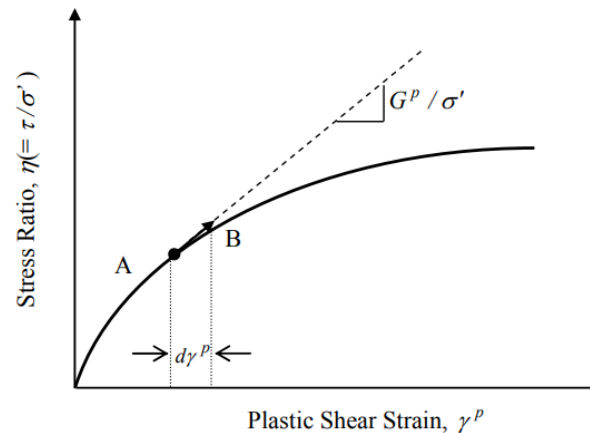


Figure 2. Plastic strain increment and plastic modulus.

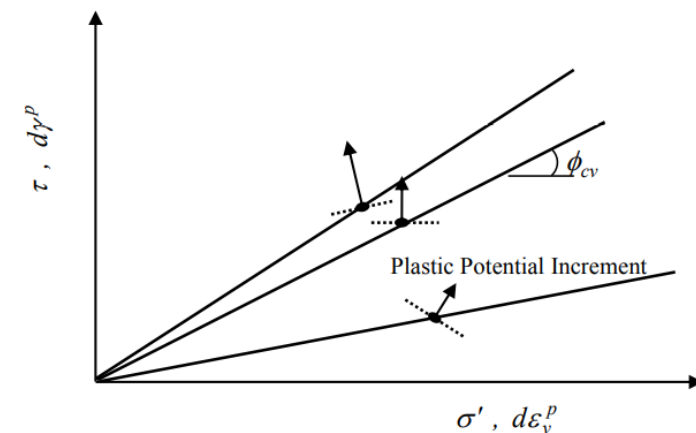


Figure 3. Directions of plastic strains associated with location of yield surface.

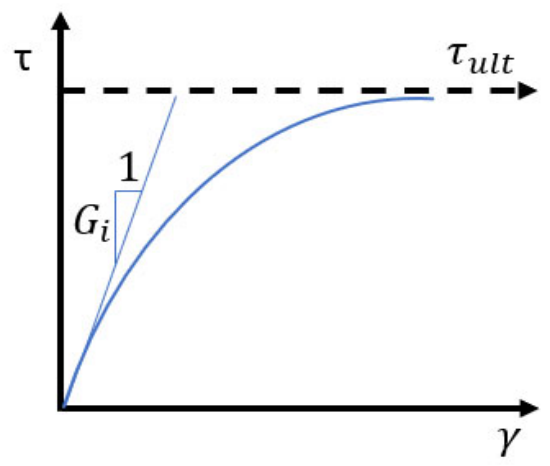
- Assumes hyperbolic response in stress ratio vs. plastic shear strain
- Plastic strains controlled by yield loci, and volume changes are predicted using the flow rule (Puebla et al. 1997)
- Plastic hardening allows volume change to accrue at decreasing rate
- UBCSAND was extended to study liquefaction of unsaturated soils (Seid-Karbasi and Byrne 2004), but assumed pore air and pore water pressures accumulate at same rate using a combined pore fluid bulk modulus



Shear Stress-Strain Hyperbolic Model

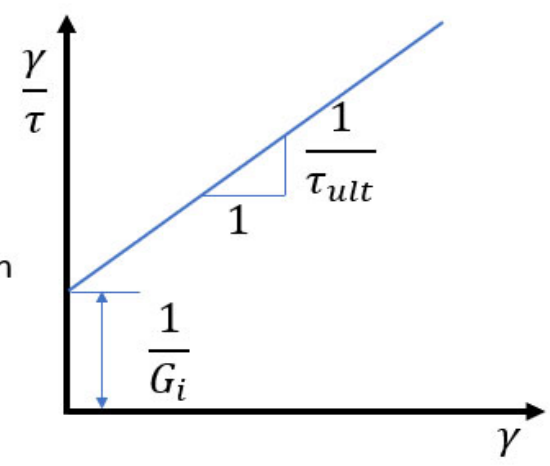
- A hyperbolic equation is used to represent the shear stress-strain curve
- The shear modulus is converted to a stress dependent parameter by linearizing the initial loading data of the shear stress shear strain curve
- By linearizing the relationship between $(\frac{\gamma}{\tau})$ and (γ) , the slope and intercept are $(\frac{1}{\tau_{ult}})$ and $(\frac{1}{G_i})$, the ultimate shear stress and initial shear modulus, respectively

$$\tau = \frac{\gamma}{\frac{1}{G_i} + \frac{\gamma}{\tau_{ult}}}$$

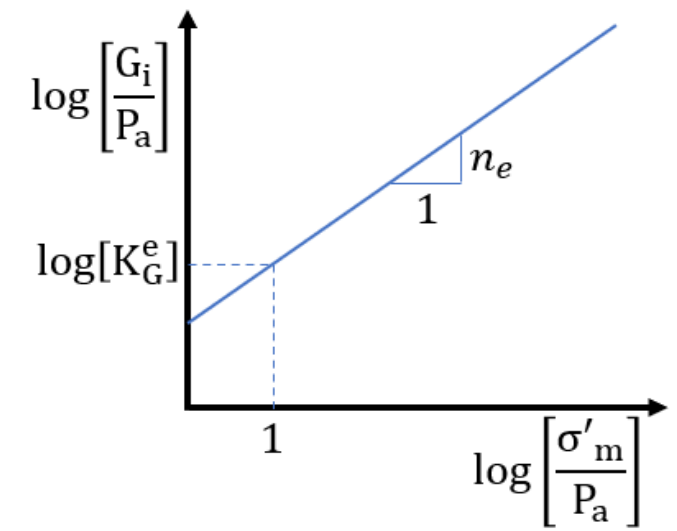


Transformation

$$\frac{\gamma}{\tau} = \frac{1}{G_i} + \frac{\gamma}{\tau_{ult}}$$

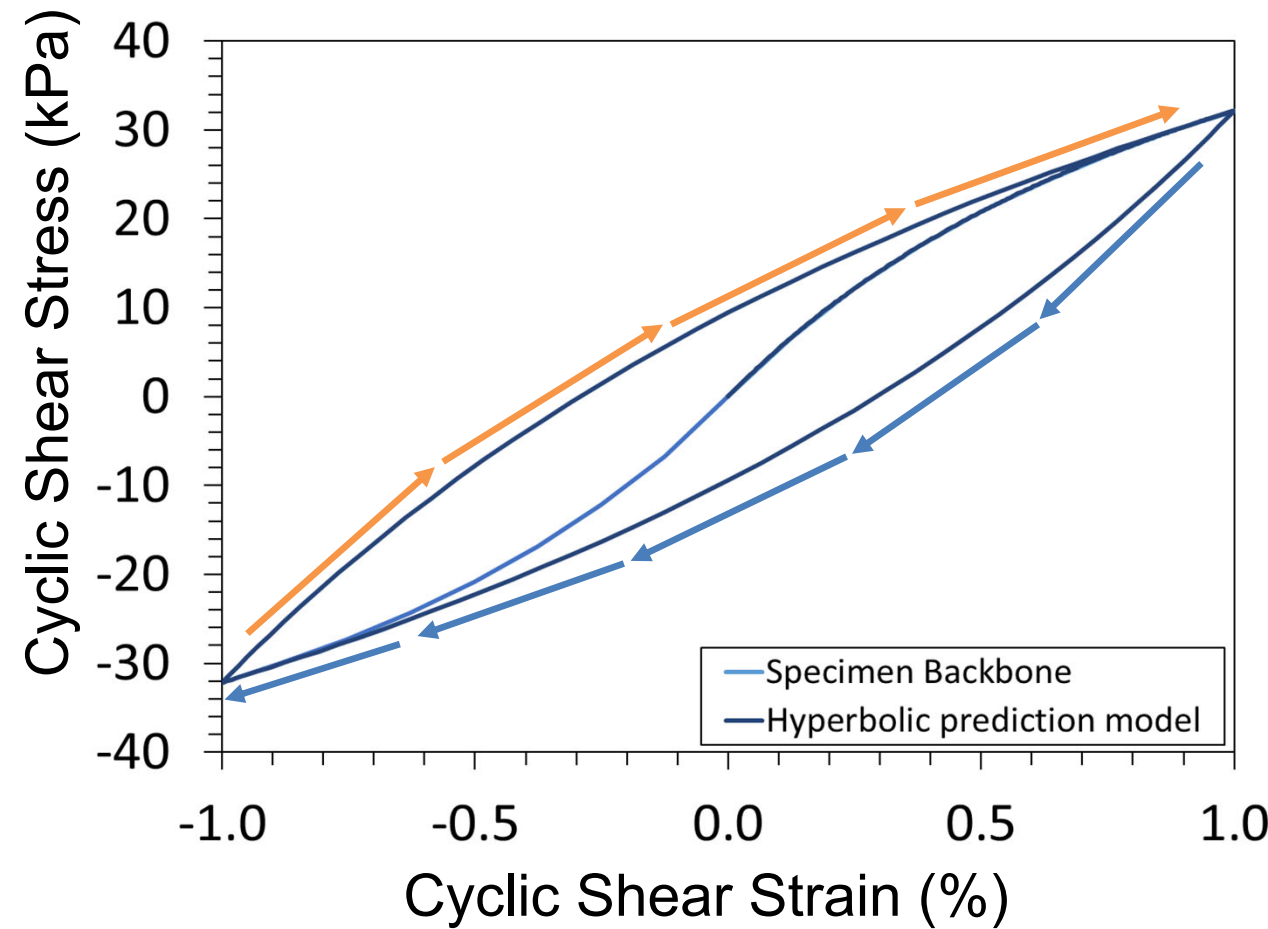


$$G_i = K_G^e * P_a * \left(\frac{\sigma'_m}{P_a}\right)^{n_e}$$





Shear Stress-Strain Hysteretic Loop



Backbone curve:

$$\tau_c = \left(\frac{\gamma_c}{\frac{1}{G_i} + \frac{\gamma_c * R_f}{\tau_{ult}}} \right)$$

Decreasing applied shear strain:

$$\tau = \left(\frac{\gamma_c - \gamma_{applied}}{\frac{1}{G_i} + \frac{(\gamma_c - \gamma_{applied}) * R_f}{2 * \tau_{ult}}} \right) + \tau_c$$

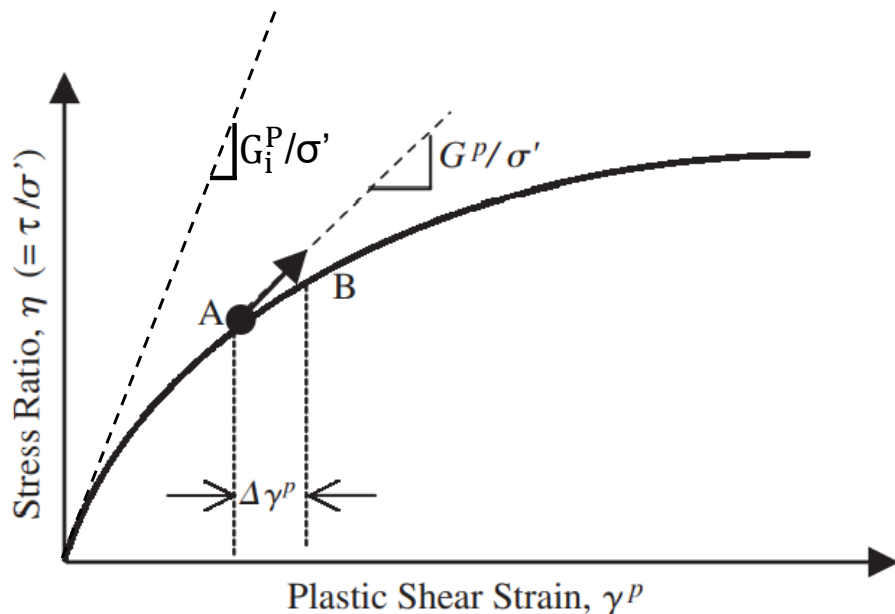
Increasing applied shear strain:

$$\tau = \left(\frac{\gamma_c + \gamma_{applied}}{\frac{1}{G_i} + \frac{(\gamma_c + \gamma_{applied}) * R_f}{2 * \tau_{ult}}} \right) - \tau_c$$



Shear Modulus in UBCSAND Model

- The initial plastic shear modulus (G_i^P) of the model when the shear stresses are low (or nearing zero) is equivalent to the elastic shear modulus
- At increasing shear stress, the normalized tangent slope of the plastic response can be predicted from the plastic shear modulus (G^P) using the shear stresses and the failure ratio calibrated from the backbone curve of the drained CSS first compression cycle (Byrne & Beatty 2011)



Small strains:

$$G_i^P = G_i = k_G^e * \left(\frac{\sigma'_m}{P_a} \right)^{n_e - 1}$$

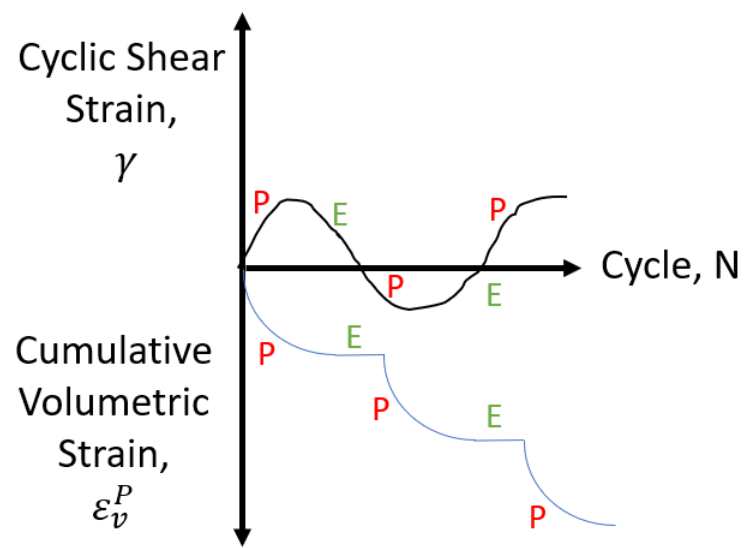
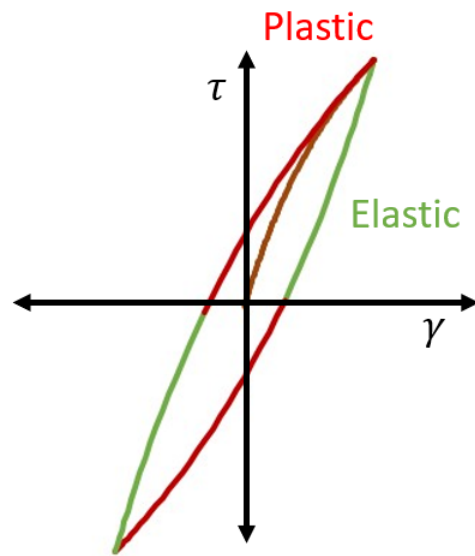
Larger strains:

$$G^P = G_i^P * \left[1 - \frac{\tau}{\tau_f} R_f \right]^{0.5}$$



Plastic Shear Strain and Volumetric Strain

- Flow rule based on energy considerations is used to compute the plastic volumetric strain response from the applied plastic shear strains (Puebla et al. 1997)
- The cumulative plastic volumetric strain (ϵ_v^p) will be the increment of each cycle plus the plastic volumetric strain from the previous cycle
- No volumetric strains occur during elastic reversals of shear strain



$$\Delta\eta_d = \left[\frac{\Delta\tau}{\sigma'_m} - \left(\frac{\tau}{(\sigma'_m)^2} \right) \Delta\sigma'_m \right]$$

$$\Delta\gamma^p = \Delta\eta_d \left(\frac{1}{G^p} \right)$$

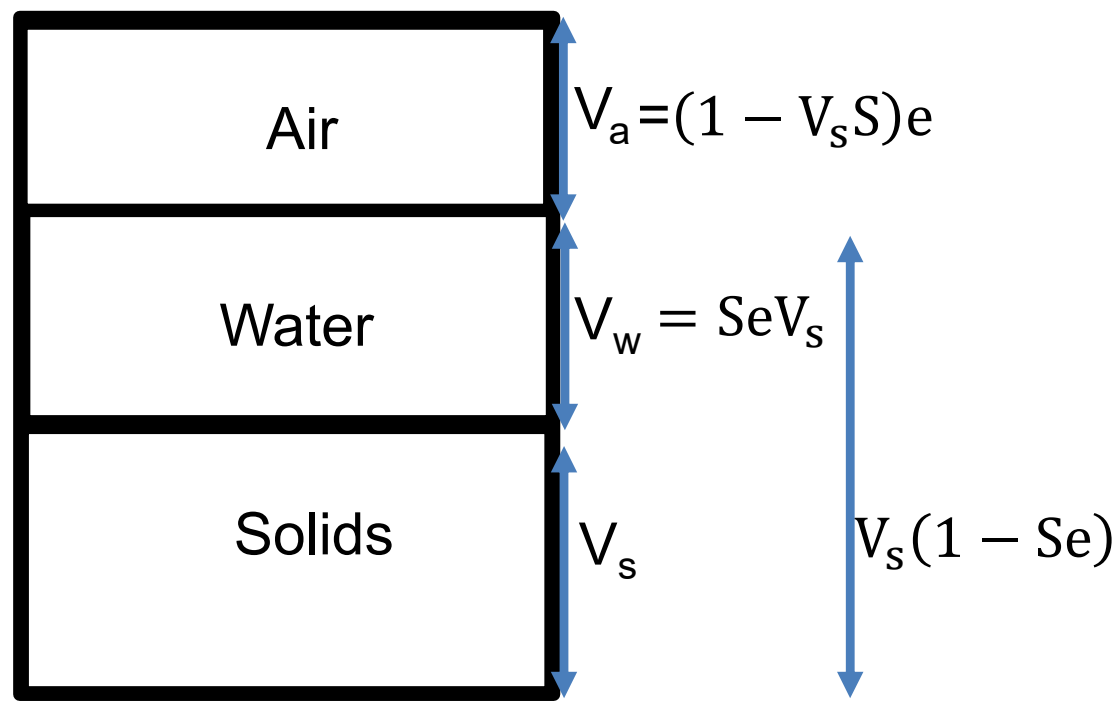
$$\Delta\epsilon_v^p = \Delta\gamma^p (\sin\phi_{cv} - \eta_d)$$

$$\epsilon_v^p = \Delta\epsilon_v^p + \epsilon_{v0}^p$$



Degree of Saturation from Volumetric Strain

$$\Delta \epsilon_v^p = \frac{\Delta V_a}{V_t}, V_t = (V_s + e_o)$$



Volume of Water and Solids:

- $S = \frac{V_w}{V_v}, e = \frac{V_v}{V_s}$
- $V_w = SeV_s$
- $V_v = V_w + V_s = V_s + SeV_s = V_s(1 + Se)$

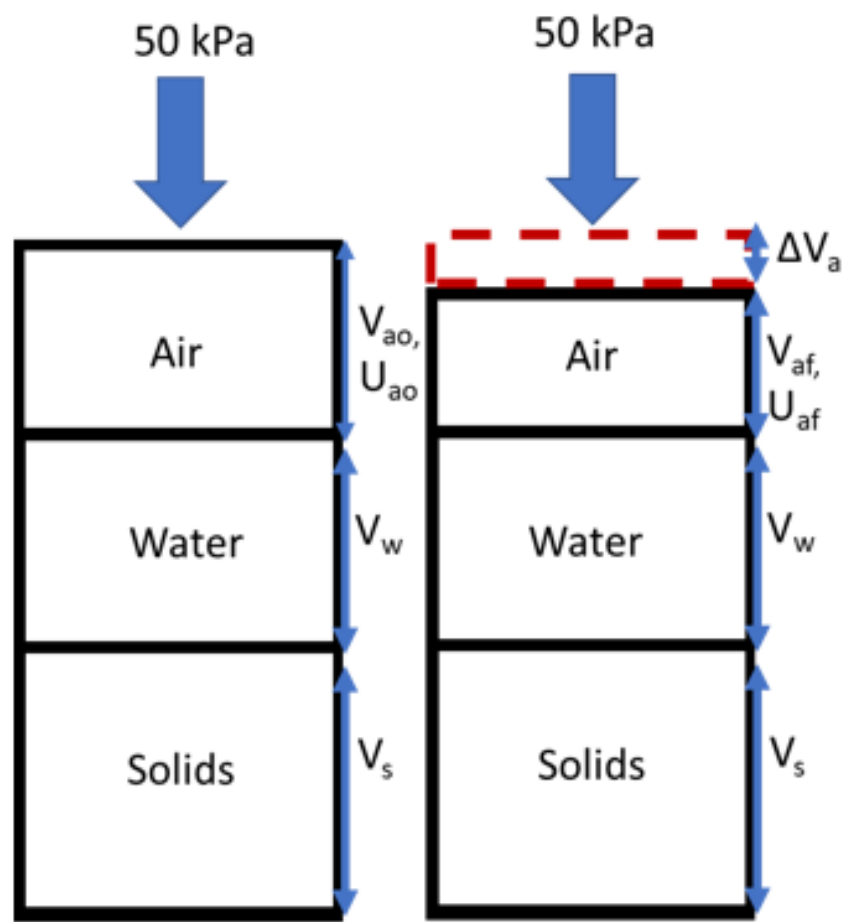
Volume of Air:

- $V_a = V_T - V_w - V_s$
- $V_a = (1 - V_s S)e$

$$S = \frac{V_s e_o S_o}{e_o - (V_s + e_o) \Delta \epsilon_v^p}$$



Pore Air Pressures during Undrained Shear



Ideal Gas Law:

$$u_{ao} V_{ao} = n_{ao(FA)} RT = \text{constant}$$

$$u_{af} V_{af} = n_{af(FA)} RT = \text{constant}$$

Boyle's Law:

$$u_{ao} V_{ao} = u_{af} V_{af}$$

$$n_{ao(DA)} = h \times u_{ao} \times V_w$$

Henry's Law:

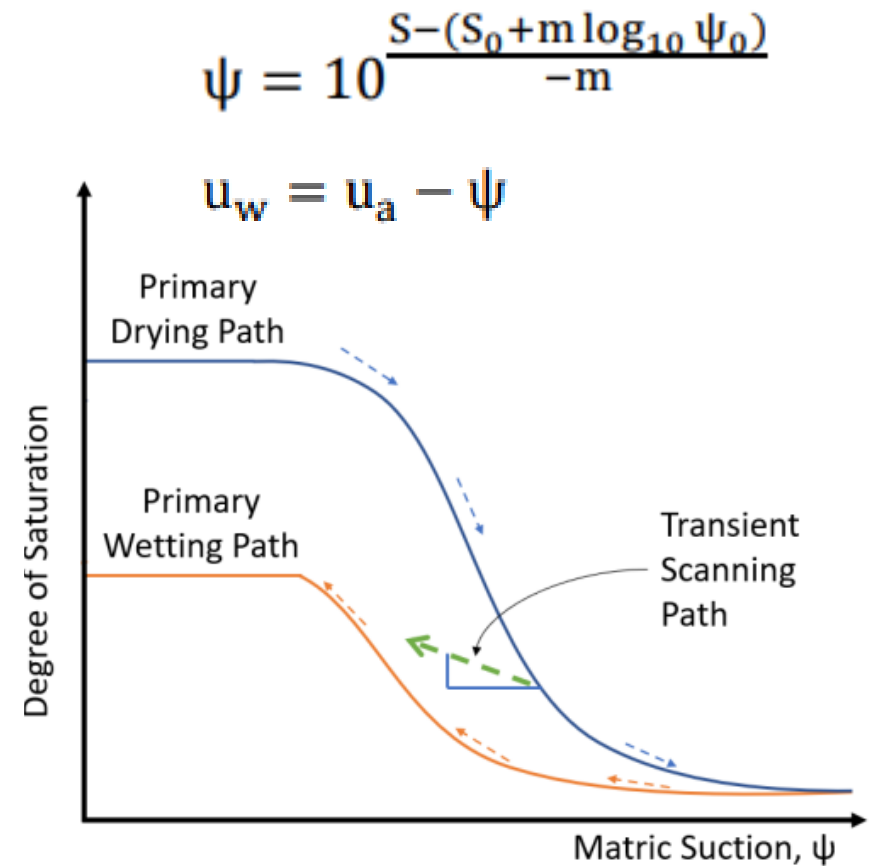
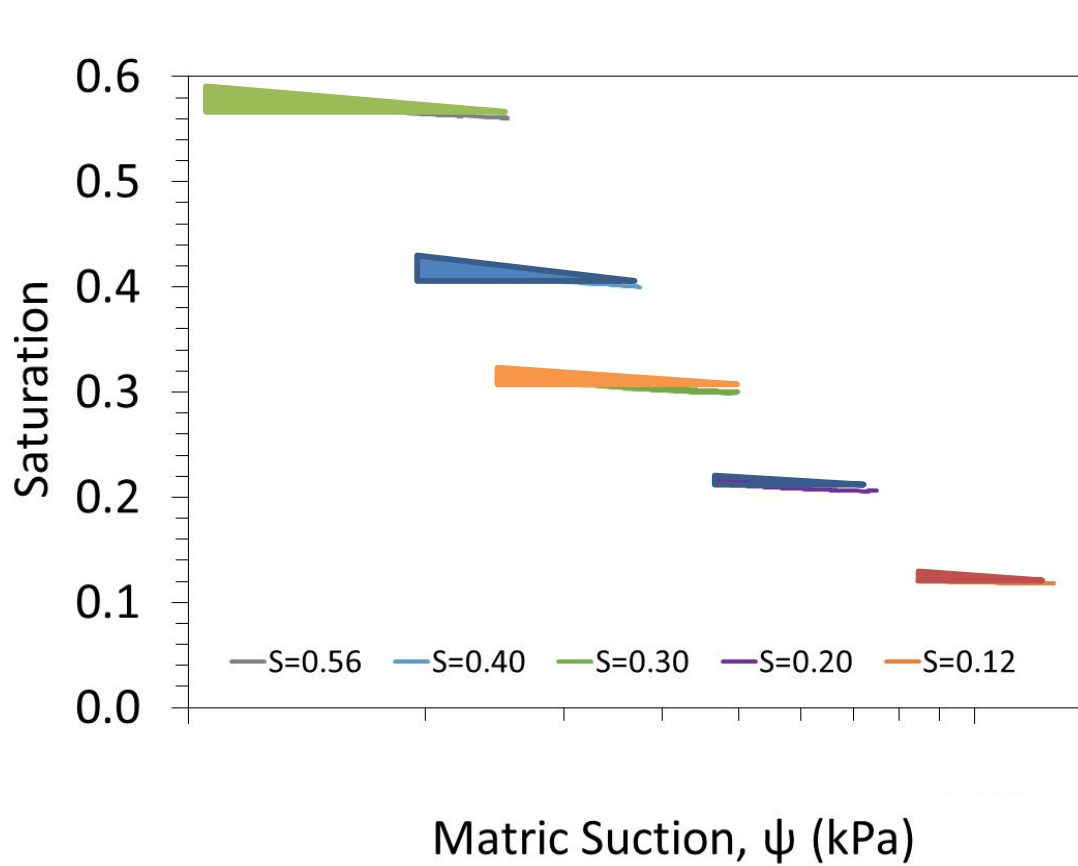
$$n_{af(DA)} = h \times u_{af} \times V_w$$

Model Equation:

$$u_a = \frac{(P_{atm} \times \epsilon_v^p (1 + e_o))}{(h \times S_o \times e_o \times RT + e_o \times (1 - S_o) - \epsilon_v^p (1 + e_o))}$$



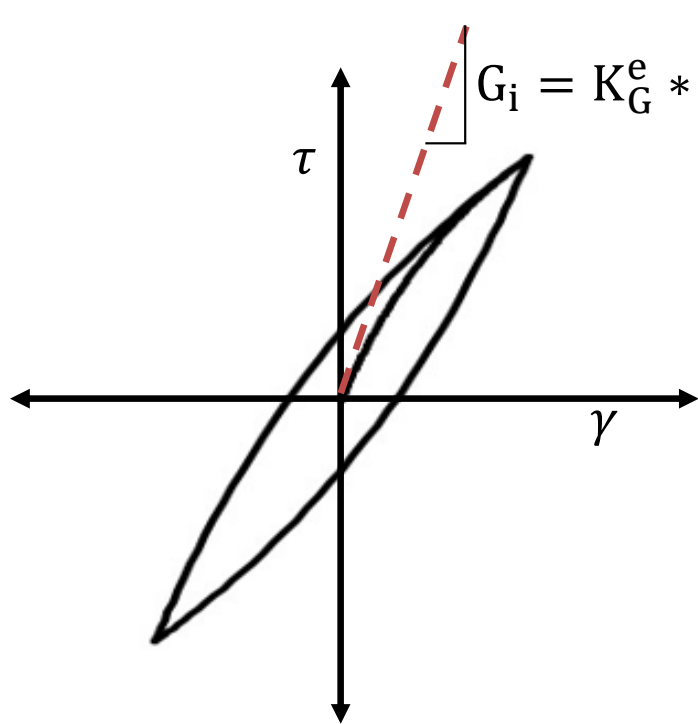
Prediction of Pore Water Pressure from the Suction on SWRC Scanning Paths



* Slope of transient SWRC scanning paths increases for higher initial saturations



Mean Effective Stress – Shear Modulus Loop



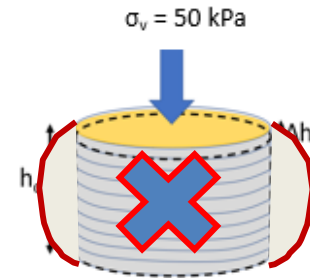
G_i and G_p are incrementally updated by the evolution in mean effective stress

Lu et al. (2010):

$$\sigma'_v = (\sigma_v - u_a) + S\psi$$

Earth pressure coefficient at rest:

$$K_o = \frac{\nu}{1 - \nu}$$



Updated mean stress:

$$\sigma'_m = \left(\frac{1 + 2K_o}{3} \right) \sigma'_v$$



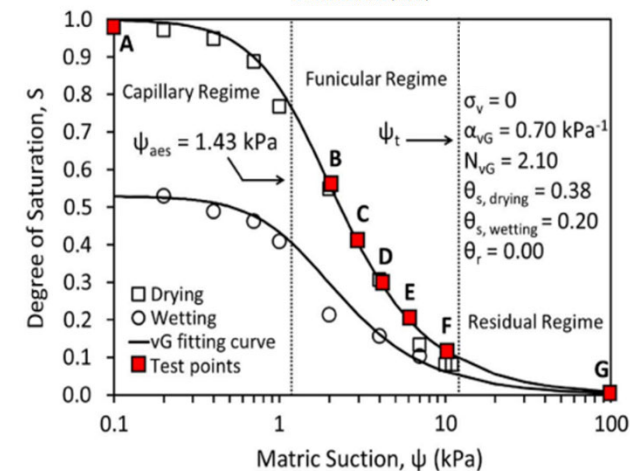
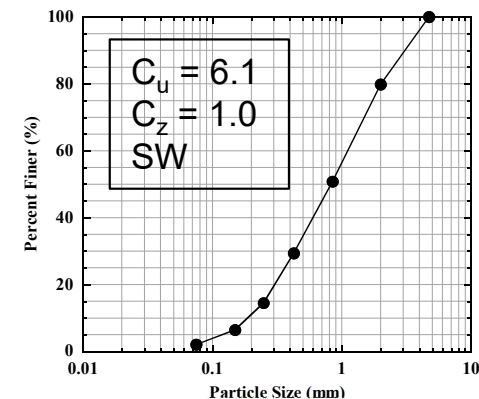
Undrained Cyclic Simple Shear Tests Simulated

McCartney and Rong (2020) Plus Preliminary Tests

Specimen No.	Initial Matric Suction ψ_o (kPa)	Initial Saturation S_o	Initial Strain Range γ_{ro} (%)	Final Strain Range γ_{rf} (%)	Intended Strain Range γ_{rn} (%)
Set 1	1.99	0.560	0.98 : (-1.00)	0.86 : (-0.95)	1.00 : (-1.00)
Set 2	1.99	0.560	0.94 : (-0.82)	1.19 : (-0.69)	1.00 : (-1.00)
Set 1	2.99	0.400	0.80 : (-0.89)	0.61 : (-1.22)	1.00 : (-1.00)
Set 2	2.99	0.400	0.88 : (-0.81)	0.51 : (-1.16)	1.00 : (-1.00)
Set 1	3.99	0.300	0.85 : (-0.94)	0.68 : (-1.04)	1.00 : (-1.00)
Set 2	3.99	0.300	0.88 : (-0.81)	0.51 : (-1.16)	1.00 : (-1.00)
Set 1*	6.00	0.206	0.89 : (-1.08)	0.83 : (-1.03)	1.00 : (-1.00)
Set 2	5.99	0.206	0.91 : (-0.72)	0.87 : (-0.82)	1.00 : (-1.00)
Set 1	9.99	0.118	1.10 : (-0.81)	1.03 : (-0.94)	1.00 : (-1.00)
Set 2	10.00	0.117	0.89 : (-1.04)	0.78 : (-1.18)	1.00 : (-1.00)
Set 1*	100.00	0	0.92 : (-1.03)	1.00 : (-0.88)	1.00 : (-1.00)
Set 2*	100.00	0	0.92 : (-0.94)	0.78 : (-1.06)	1.00 : (-1.00)

Note: The dry specimen is assumed to have a suction value of 100 kPa.

*Unpublished data



- All valves closed during undrained conditions
- Generation of pore air and water pressures results in reduction of mean stress
- Volumetric contraction leads to an increase in the degree of saturation

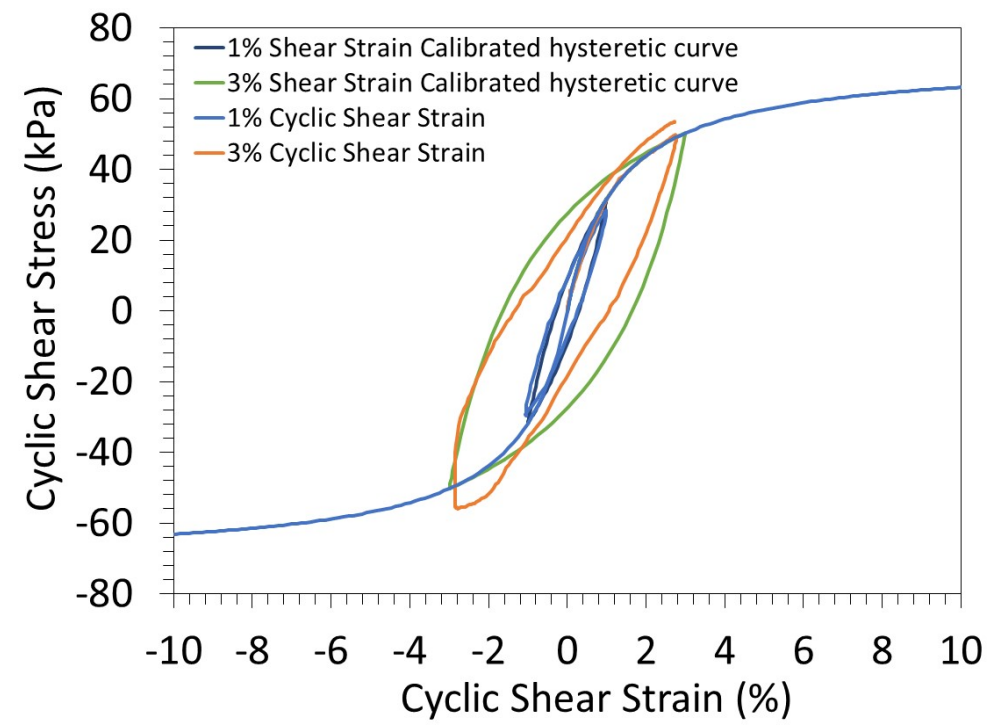


Calibrated Backbone Curve Shape Parameters

Peak friction angle and constant volume friction angle obtained from triaxial compression tests of Zheng et al. (2018)

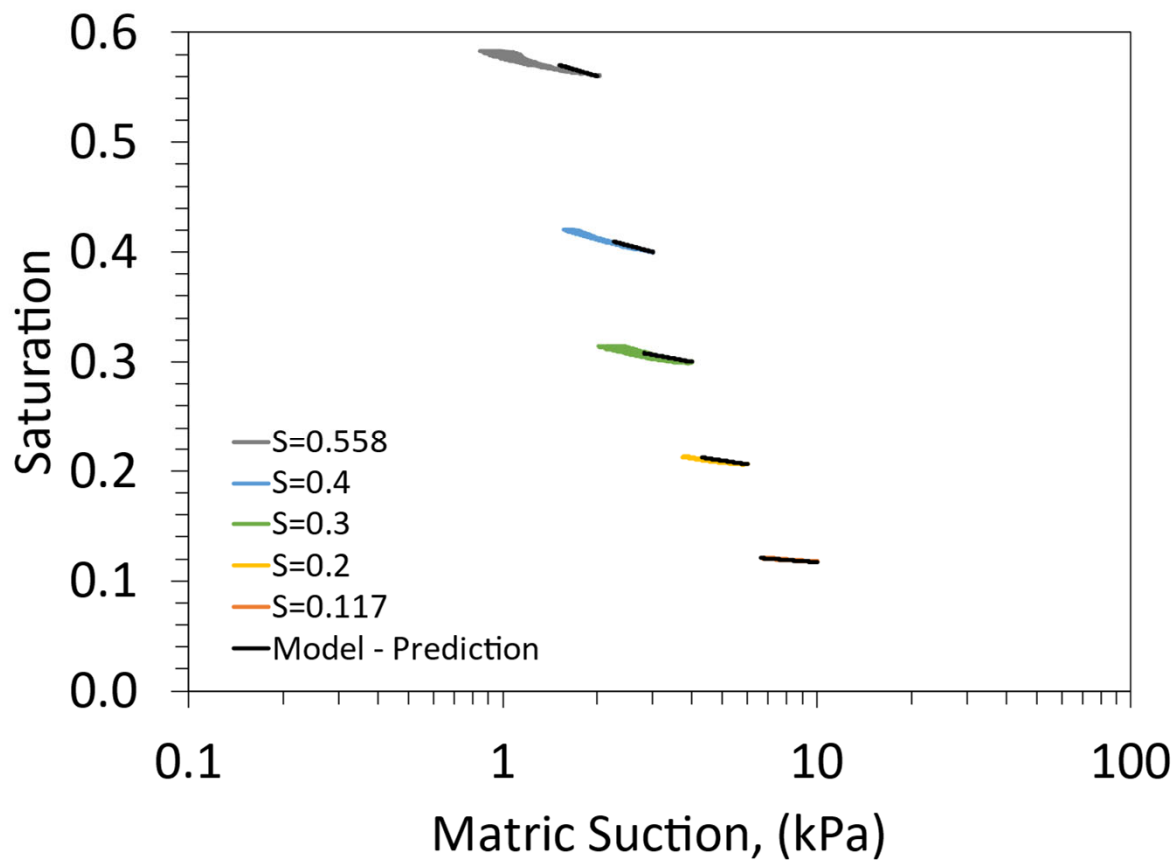
Average calibrated parameters for the hyperbolic model from drained cyclic simple shear tests of Rong and McCartney (2020)

e_o	n_e	K_e^G	R_f	ϕ'_{cv} (Deg)	ϕ'_p (Deg)
0.636	0.49	100	0.9	34.0	51.3

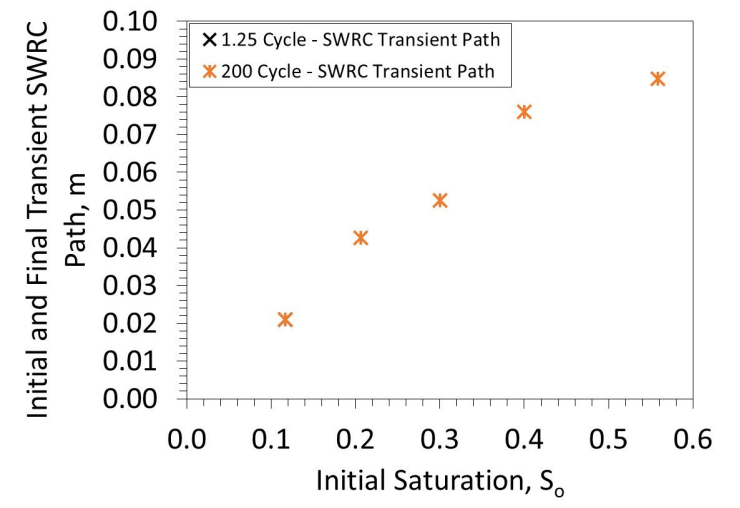




Calibration of Transient SWRC Scanning Path



$$m = 0.021 + 0.14 \times S_0$$



Changes in the slope of the transient SWRC scanning paths with initial degree of saturation were well-captured with a linear relationship

S_0	m_{final}
0.117	0.021
0.206	0.043
0.300	0.053
0.400	0.075
0.560	0.085



Summary of Model Inputs and Parameters

Shear Stress - Shear Strain and Effective Stress Equation Parameters

e_o	σ_v (kPa)	ν	K_o	n_e	K_e^G	R_f	ϕ'_{cv} (Deg)	ϕ'_p (Deg)
0.636	50	0.33	0.5	0.49	100	0.9	34.0	51.3

Pore Air Pressure Constants

P_{air} (kg/m ³)	P_{water} (kg/m ³)	R ($\frac{Nm}{mol K}$)	K (Kelvin)
1.204	998.19	8.314	294.3

Parameters for Evolution in
Transient SWRC Path Slope
with Initial Degree of
Saturation

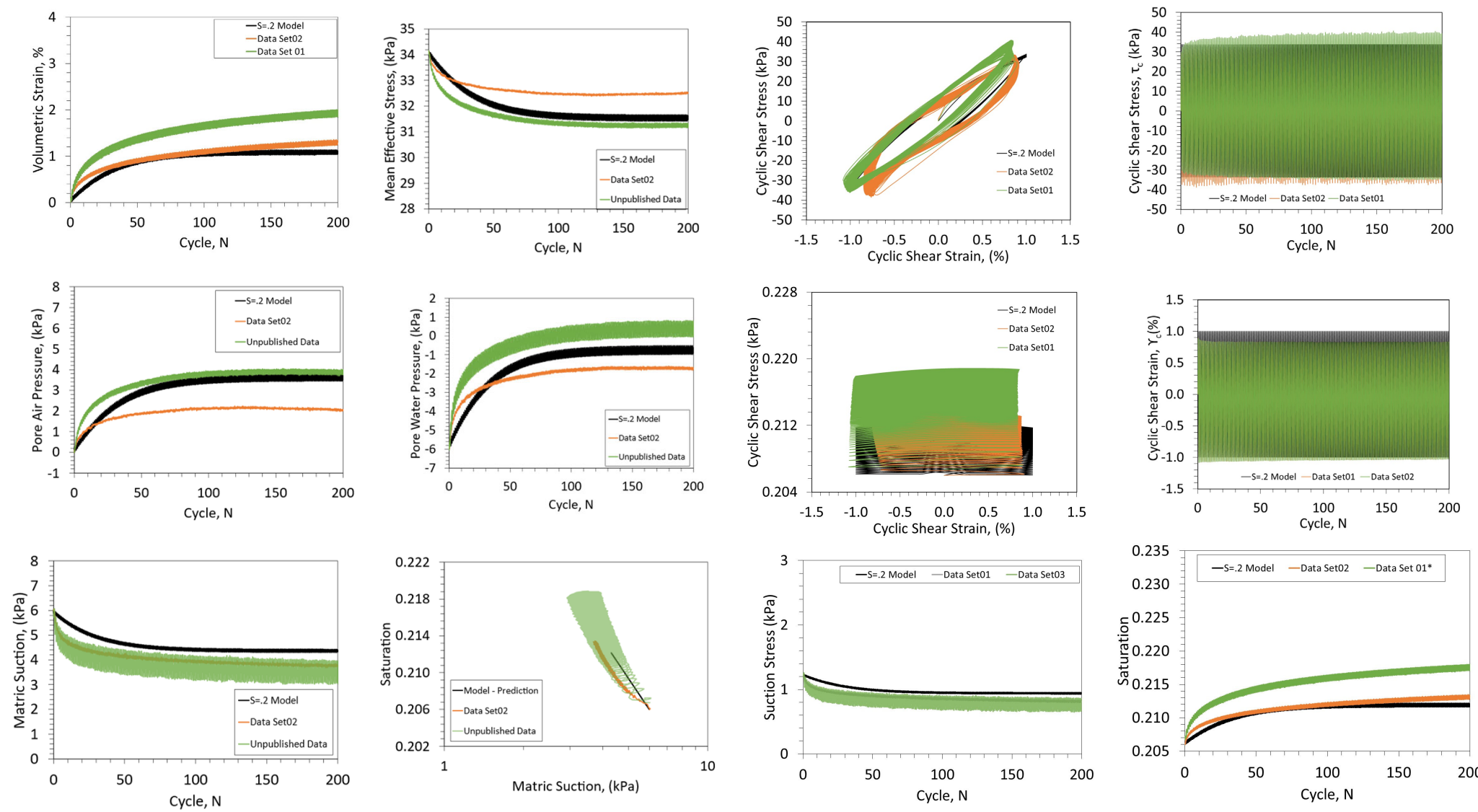
$$m = 0.021 + 0.14 \times S_0$$

Cyclic loading conditions (input)

γ_c (%)	f (Hz)
1	1

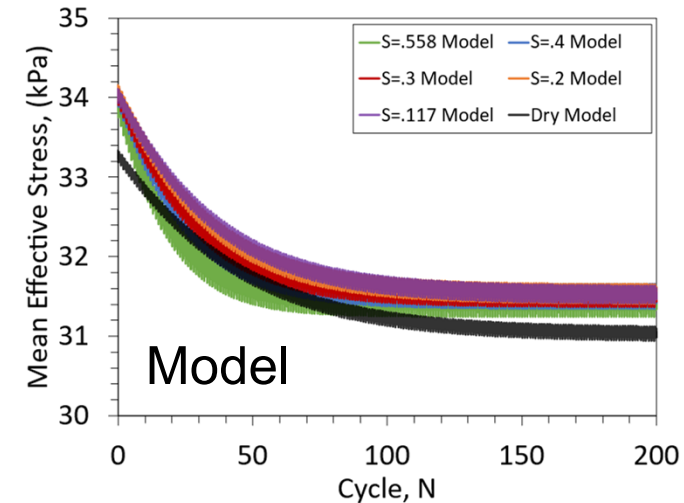
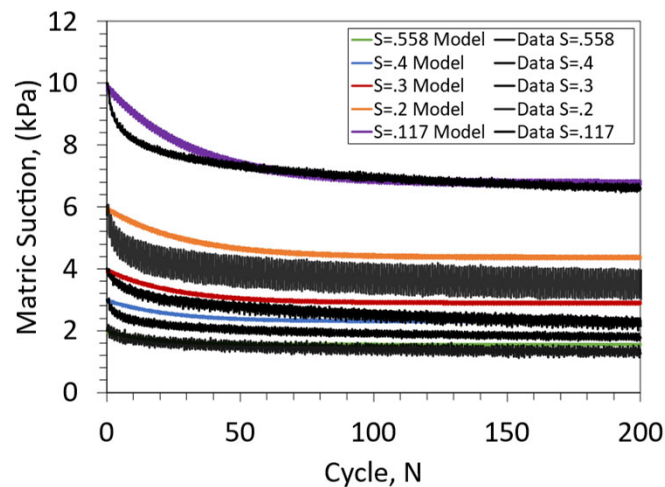
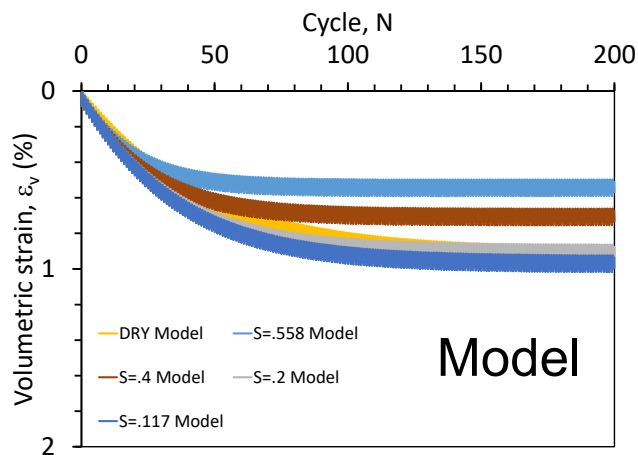
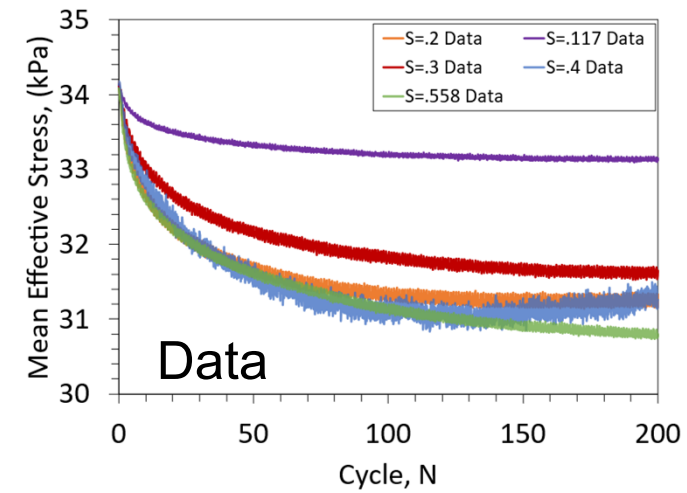
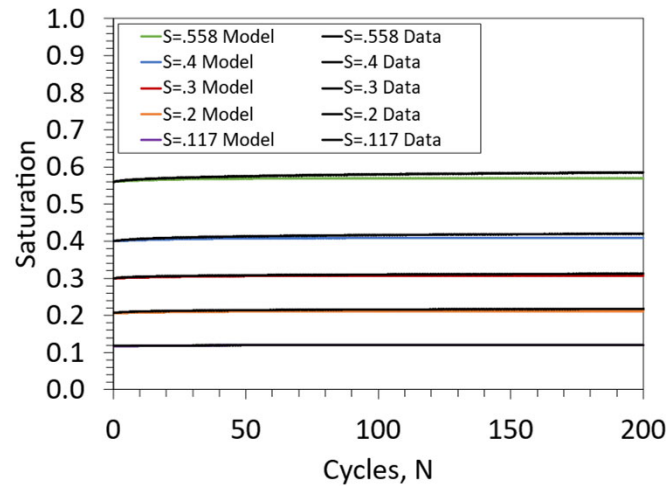
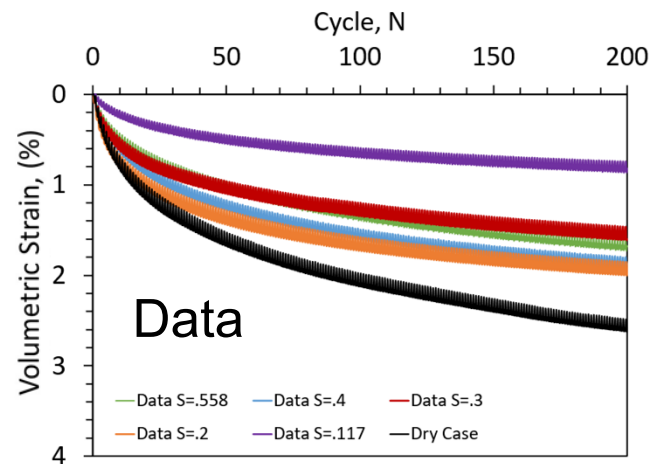


Example of Model Validation: $\psi_o = 6 \text{ kPa}$, $S_o = 0.2$



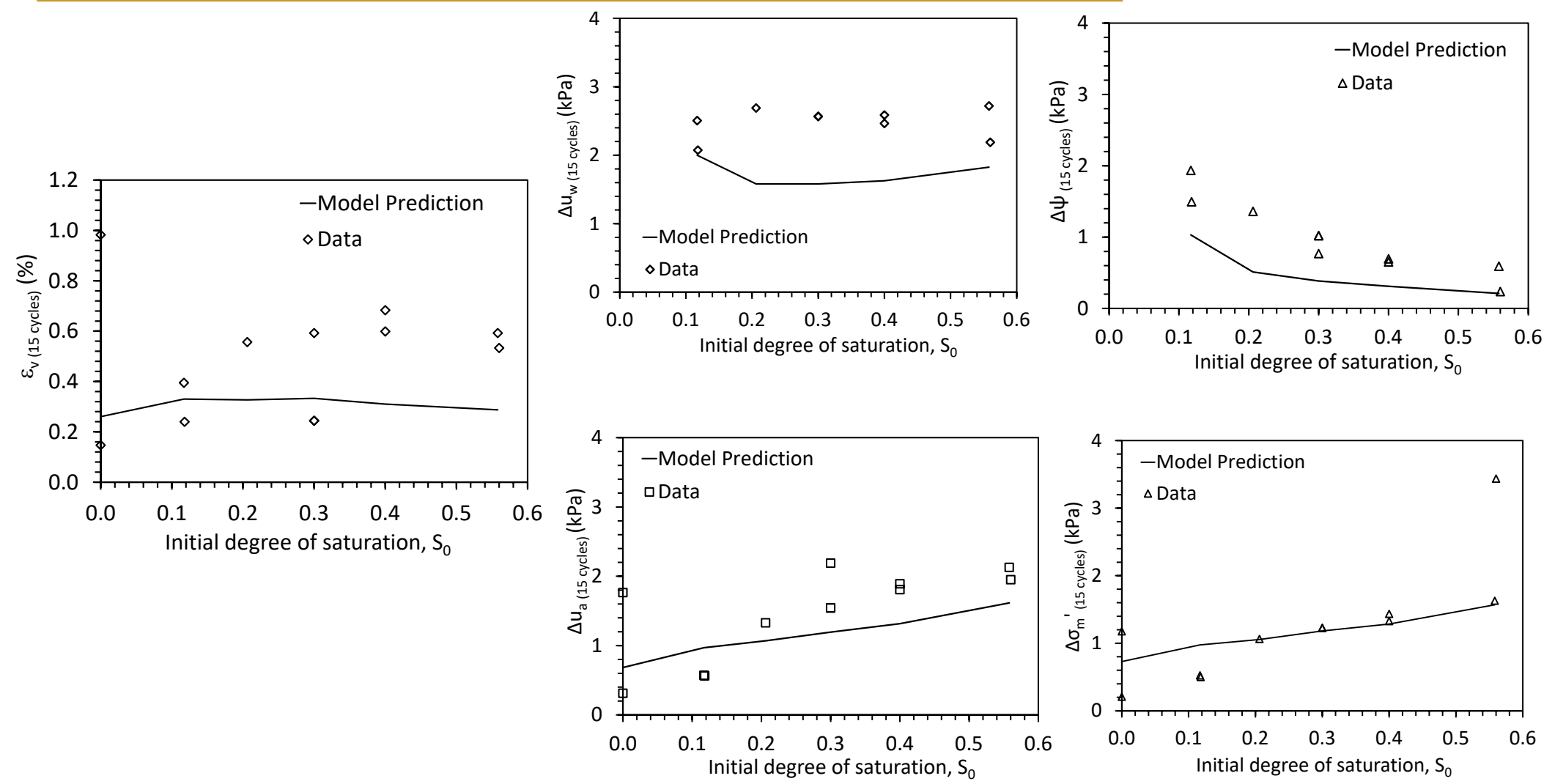


Evaluation of Effects of Initial Degree of Saturation on Seismic Compression





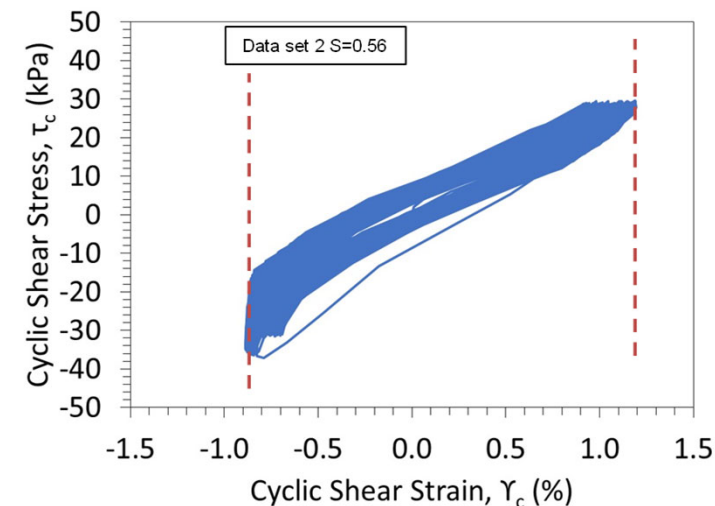
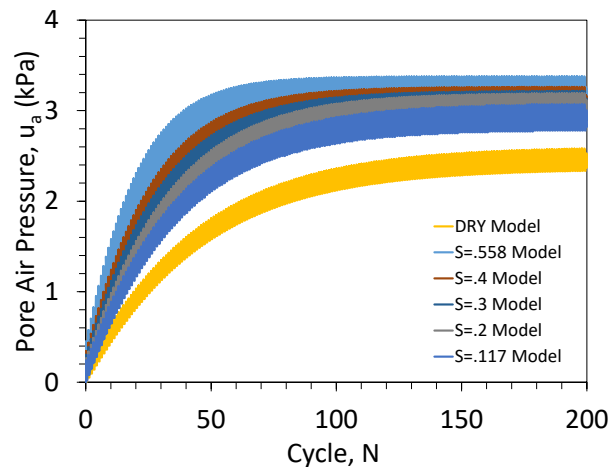
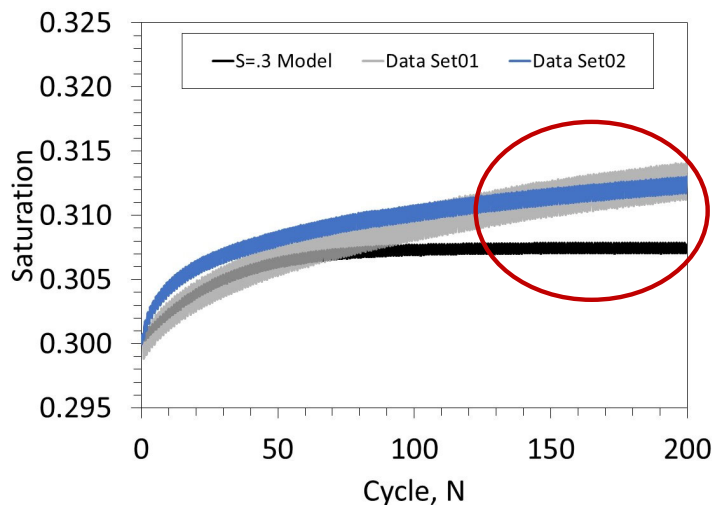
Synthesis of Model Results: 15 Cycles





Possible Reasons behind Discrepancies between Model and Experiments

- Model could not capture the effects of changes in peak cyclic shear strain during application of large numbers of cycles (model stabilizes but experiments do not)
 - Possible creep mechanism in addition to hydro-mechanical effects
 - Pore air pressures for different initial degrees of saturation are similar at large numbers of cycles
- Experimental issues may partly explain discrepancy (drift in hysteresis loops, redistribution of pore water, shape of stress-strain loops, not between $\pm 1\%$)





Conclusions

- Model performed reasonably for small numbers of cycles
 - Captured transient changes in hydro-mechanical variables during undrained cyclic shearing in the funicular regime
 - Permanent volumetric compressions in cyclic simple shear tests are underpredicted
- Use of unsaturated soil mechanics permits tracking of stress state during cyclic shearing under different drainage conditions
 - Linkage between effective stress and dynamic properties
 - Seismic compression is an elasto-plastic process
- Future research needs:
 - Extend the model beyond the funicular regime: consider post-liquefaction consolidation
 - Better understand the roles of parameter n (vertical stress effects), initial relative density, cyclic shear strain amplitude